Extreme value statistics and the largest structures in the Universe

Stéphane Colombi

Institut d'Astrophysique de Paris

Note : extreme value statistics are a big deal !
A journal is dedicated to them !

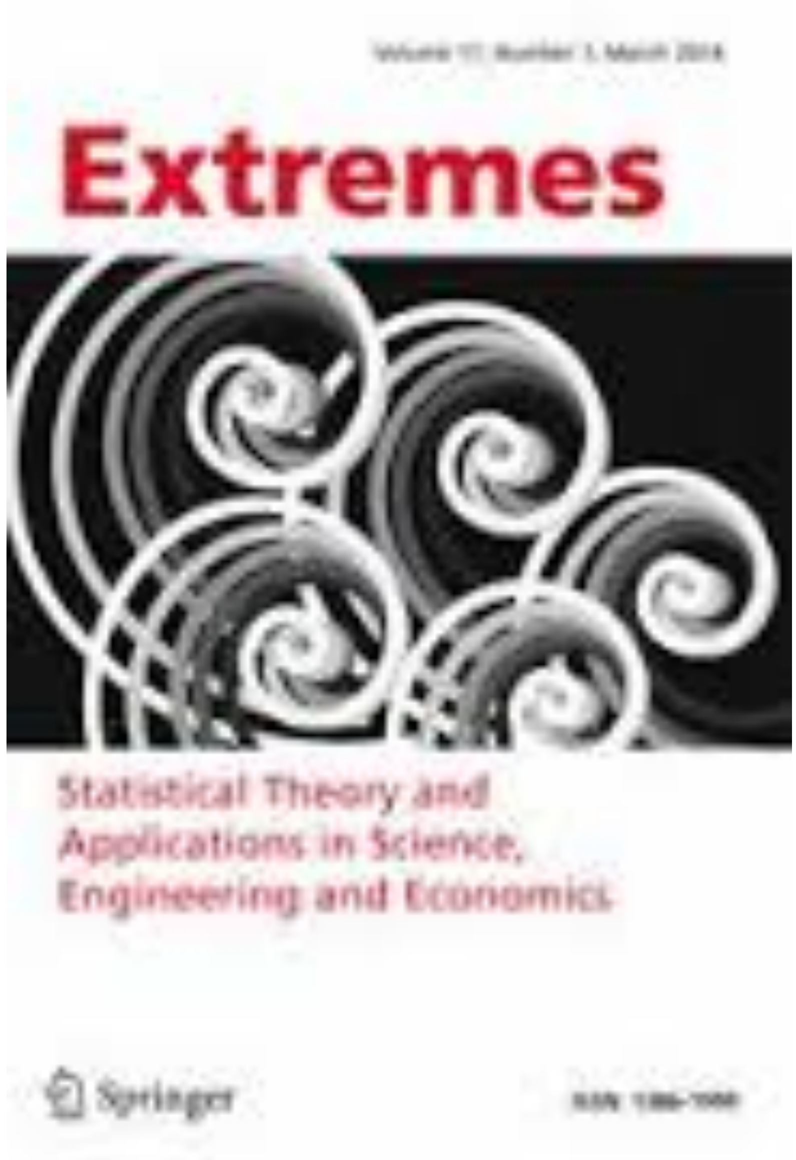

The large scale galaxy distribution

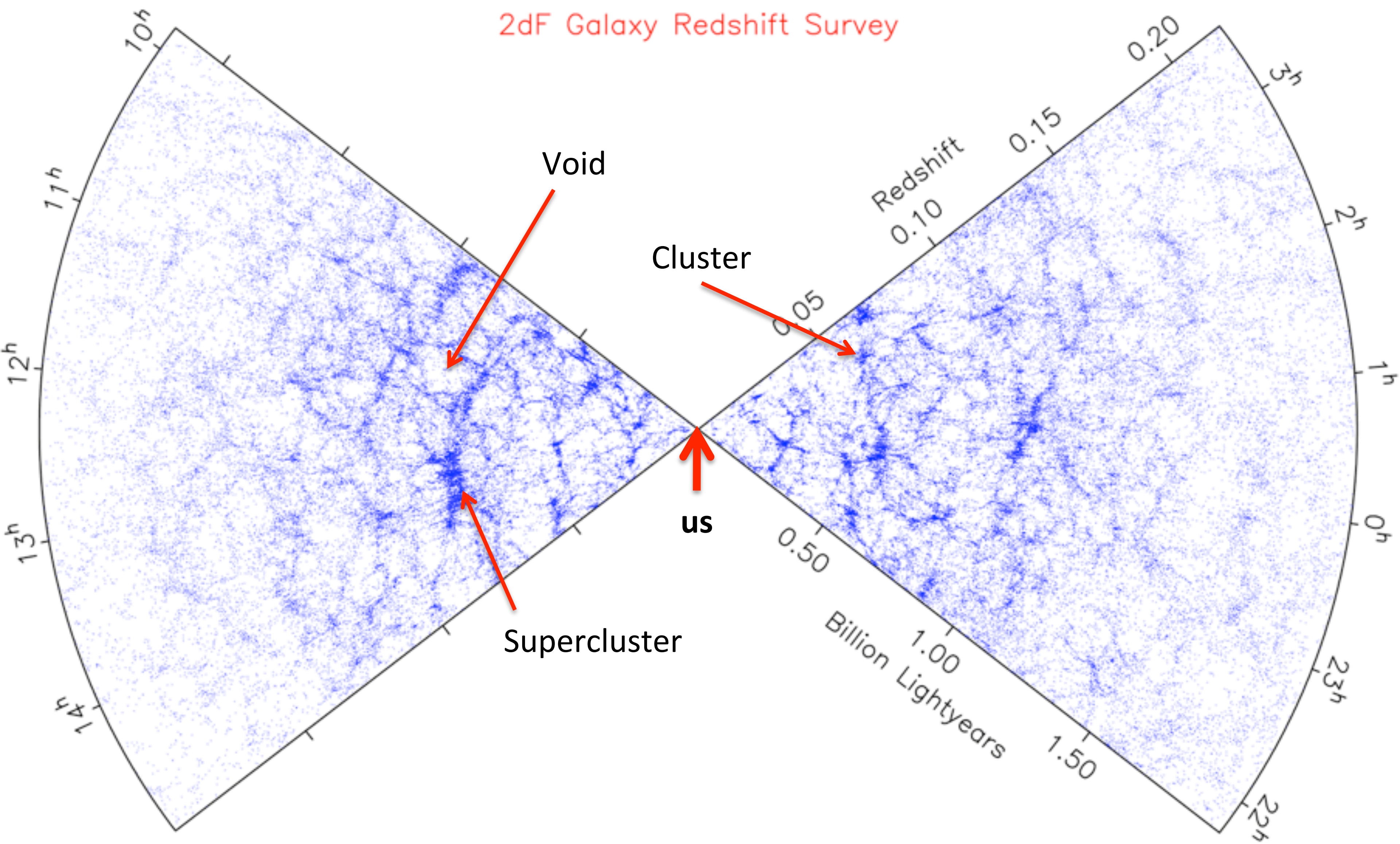

Galaxies in the SDSS

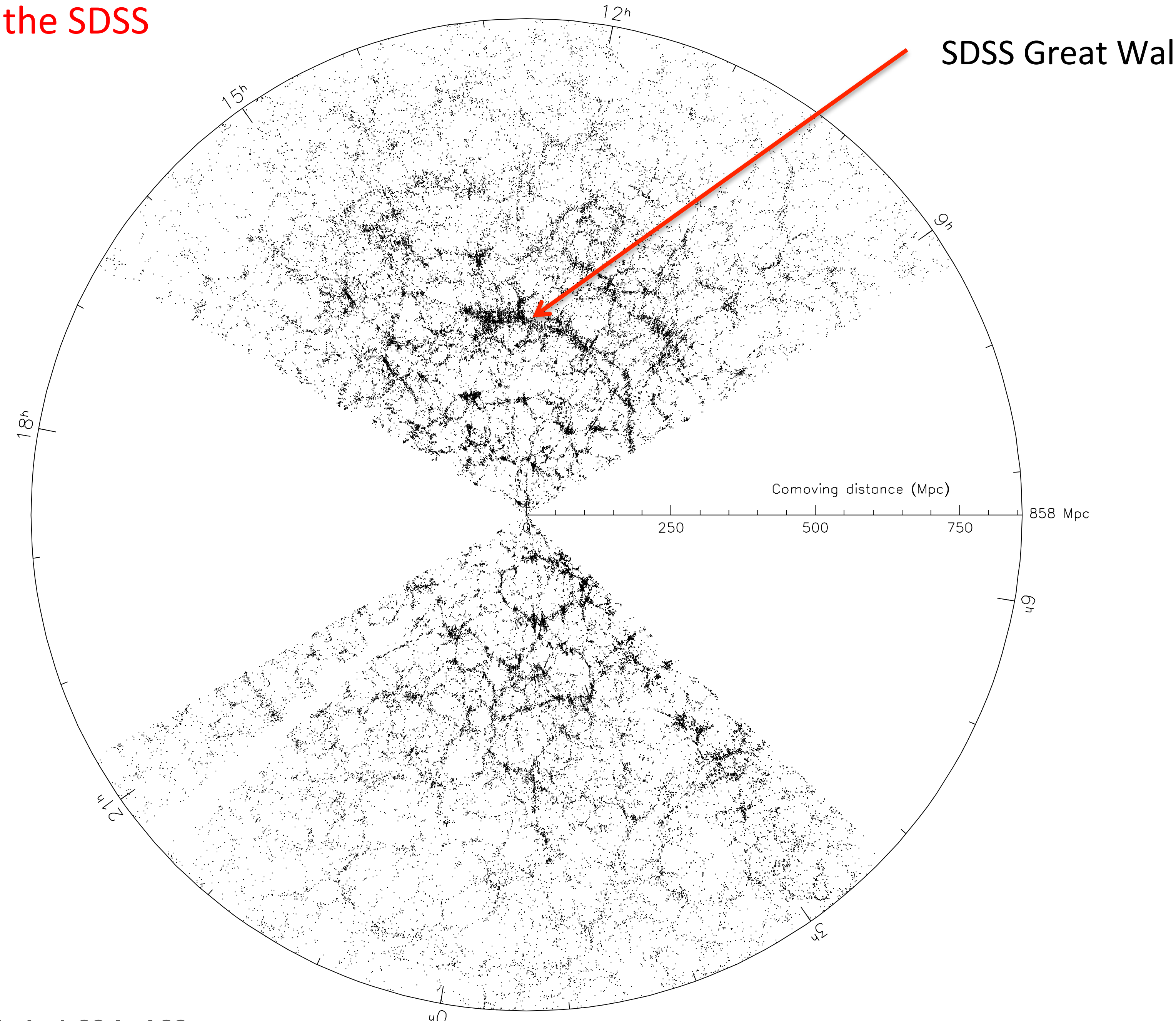

Gott et al. 2005, ApJ 624, 463

THE ASTROPHYSICAL JOURNAL, 302:L1–L5, 1986 March 1

A SLICE OF THE UNIVERSE[1]

VALÉRIE DE LAPPARENT,[2,3] MARGARET J. GELLER,[2] AND JOHN P. HUCHRA[2]
Received 1985 November 12; accepted 1985 December 5

ABSTRACT

We describe recent results obtained as part of the extension of the Center for Astrophysics redshift survey to $m_B = 15.5$. The new sample contains 1100 galaxies (we measured 584 new redshifts) in a $6° \times 117°$ strip going through the Coma cluster. Several features of the data are striking. The galaxies appear to be on the surfaces of bubble-like structures. The bubbles have a typical diameter of $\sim 25h^{-1}$ Mpc. The largest bubble in the survey has a diameter of $\sim 50h^{-1}$ Mpc, comparable with the most recent estimates of the diameter of the void in Bootes. The galaxy density in the region of the largest void contained in the survey is only 0.20 of the mean. The edge of the largest void in the survey is remarkably sharp.

All of these features pose serious challenges for current models for the formation of large-scale structure. The best available model for generating these structures is the explosive galaxy formation theory of Ostriker and Cowie, published in 1981. These new data might be the basis for a new picture of the galaxy and cluster distributions.

Subject headings: cosmology — galaxies: clustering — galaxies: formation

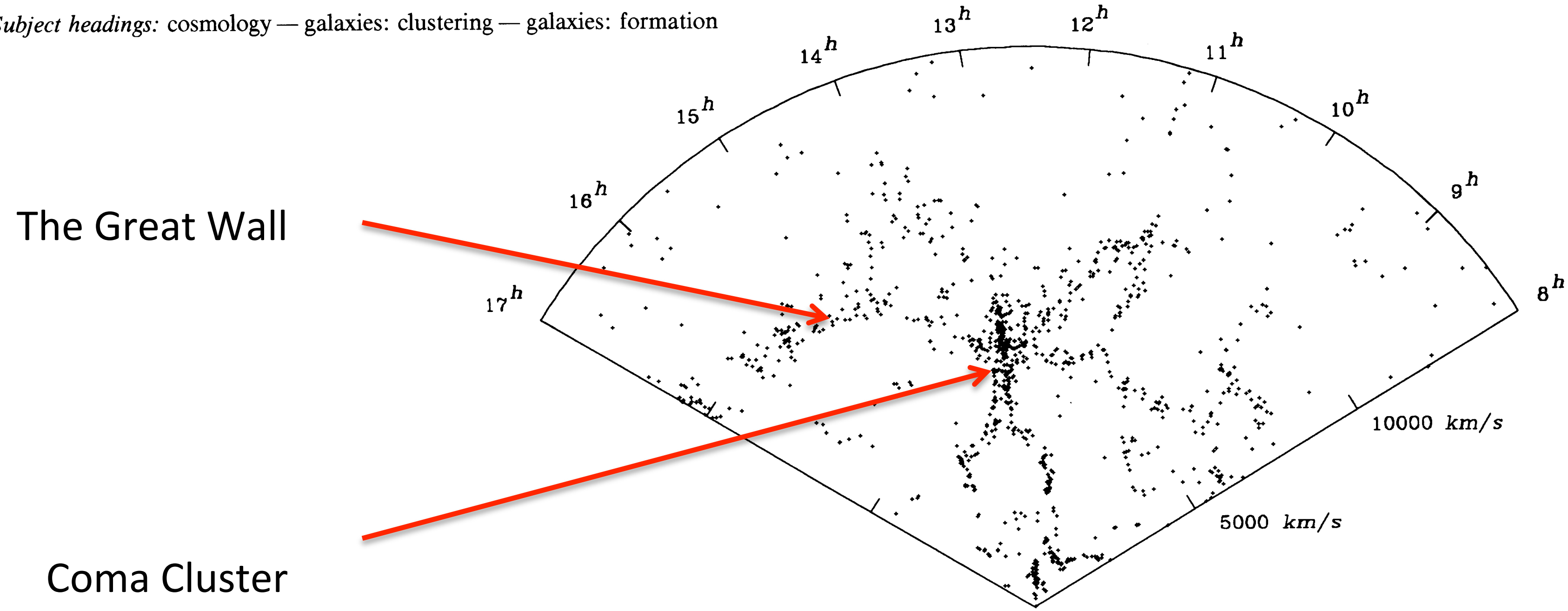

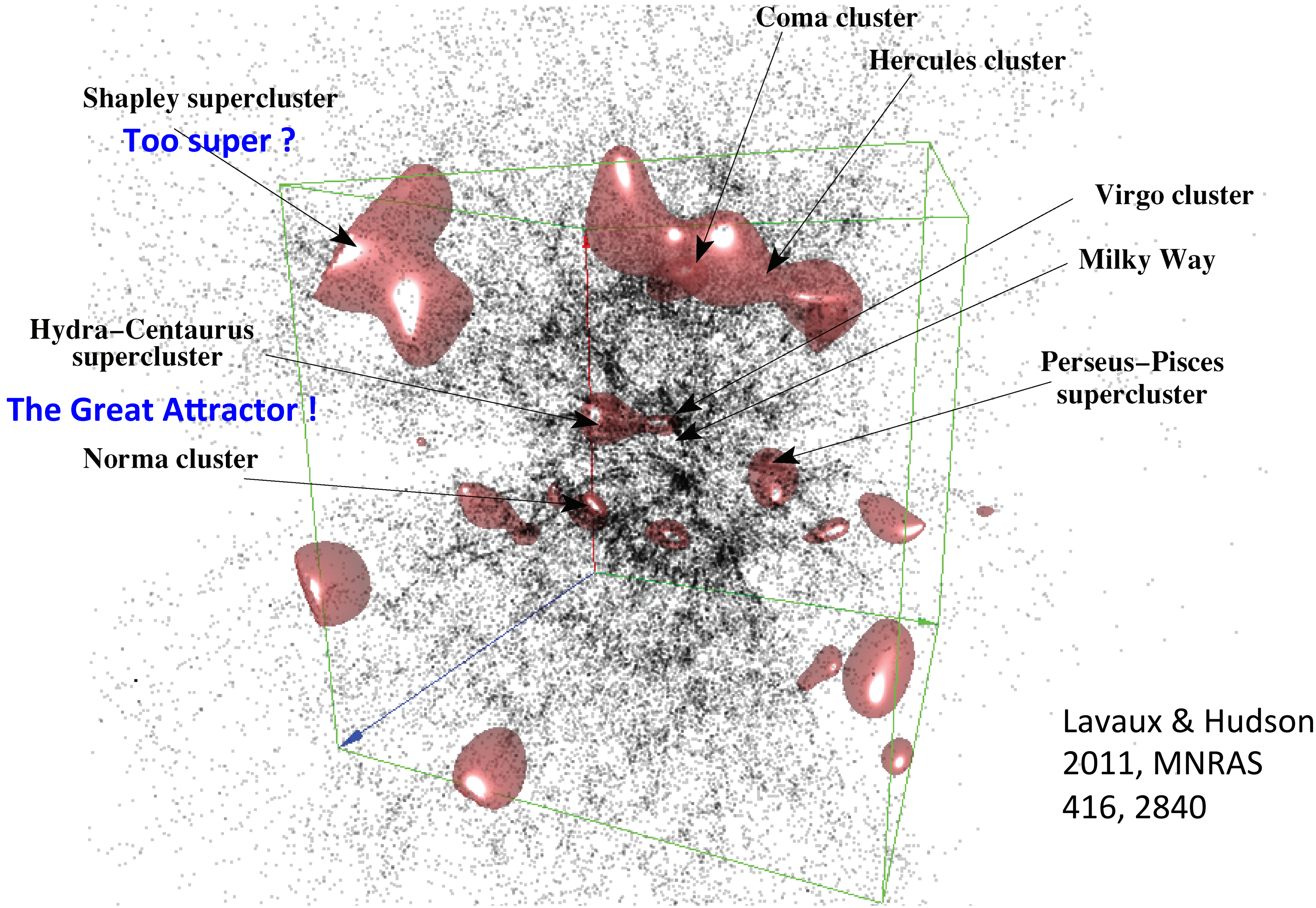

Figure 13. The 2M++ galaxy distribution and density field in three dimensions. The cube frame is in Galactic coordinates. The Galactic plane cuts orthogonally through the middle of the back vertical red arrow. The length of a side of the cube is 200 h^{-1} Mpc and is centred on Milky Way. We highlight the isosurface of number fluctuation, smoothed with a Gaussian kernel of radius 1000 km s^{-1}, $\delta_L = 2$ with a shiny dark red surface. The positions of some major structures in the local Universe are indicated by labelled arrows. We do not show isosurfaces beyond a distance of 150 h^{-1} Mpc, so HR is, for example, not present.

El Gordo !

THE ATACAMA COSMOLOGY TELESCOPE: ACT-CL J0102−4915 "EL GORDO," A MASSIVE MERGING CLUSTER AT REDSHIFT 0.87

Felipe Menanteau[1], John P. Hughes[1], Cristóbal Sifón[2], Matt Hilton[3], Jorge González[2], Leopoldo Infante[2], L. Felipe Barrientos[2], Andrew J. Baker[1], John R. Bond[4], Sudeep Das[5,6,7], Mark J. Devlin[8], Joanna Dunkley[9], Amir Hajian[4], Adam D. Hincks[7], Arthur Kosowsky[10], Danica Marsden[8], Tobias A. Marriage[11], Kavilan Moodley[12], Michael D. Niemack[13], Michael R. Nolta[4], Lyman A. Page[7], Erik D. Reese[8], Neelima Sehgal[14], Jon Sievers[4], David N. Spergel[6], Suzanne T. Staggs[7], and Edward Wollack[15]

ABSTRACT

We present a detailed analysis from new multi-wavelength observations of the exceptional galaxy cluster ACT-CL J0102−4915, likely the most massive, hottest, most X-ray luminous and brightest Sunyaev–Zel'dovich (SZ) effect cluster known at redshifts greater than 0.6. The Atacama Cosmology Telescope (ACT) collaboration discovered ACT-CL J0102−4915 as the most significant SZ decrement in a sky survey area of 755 deg^2. Our Very Large Telescope (VLT)/FORS2 spectra of 89 member galaxies yield a cluster redshift, $z = 0.870$, and velocity dispersion, $\sigma_{\rm gal} = 1321 \pm 106$ km s^{-1}. Our *Chandra* observations reveal a hot and X-ray luminous system with an integrated temperature of $T_{\rm X} = 14.5 \pm 0.1$ keV and 0.5–2.0 keV band luminosity of $L_{\rm X} = (2.19 \pm 0.11) \times 10^{45}\, h_{70}^{-2}$ erg s^{-1}. We obtain several statistically consistent cluster mass estimates; using empirical mass scaling relations with velocity dispersion, X-ray $Y_{\rm X}$, and integrated SZ distortion, we estimate a cluster mass of $M_{200a} = (2.16 \pm 0.32) \times 10^{15}\, h_{70}^{-1}\, M_\odot$. We constrain the stellar content of the cluster to be less than 1% of the total mass, using *Spitzer* IRAC and optical imaging. The *Chandra* and VLT/FORS2 optical data also reveal that ACT-CL J0102−4915 is undergoing a major merger between components with a mass ratio of approximately 2 to 1. The X-ray data show significant temperature variations from a low of 6.6 ± 0.7 keV at the merging low-entropy, high-metallicity, cool core to a high of 22 ± 6 keV. We also see a wake in the X-ray surface brightness and deprojected gas density caused by the passage of one cluster through the other. Archival radio data at 843 MHz reveal diffuse radio emission that, if associated with the cluster, indicates the presence of an intense double radio relic, hosted by the highest redshift cluster yet. ACT-CL J0102−4915 is possibly a high-redshift analog of the famous Bullet cluster. Such a massive cluster at this redshift is rare, although consistent with the standard ΛCDM cosmology in the lower part of its allowed mass range. Massive, high-redshift mergers like ACT-CL J0102−4915 are unlikely to be reproduced in the current generation of numerical *N*-body cosmological simulations.

Key words: cosmic background radiation – cosmology: observations – galaxies: clusters: general – galaxies: clusters: individual (ACT-CL J0102−4915)

Online-only material: color figures

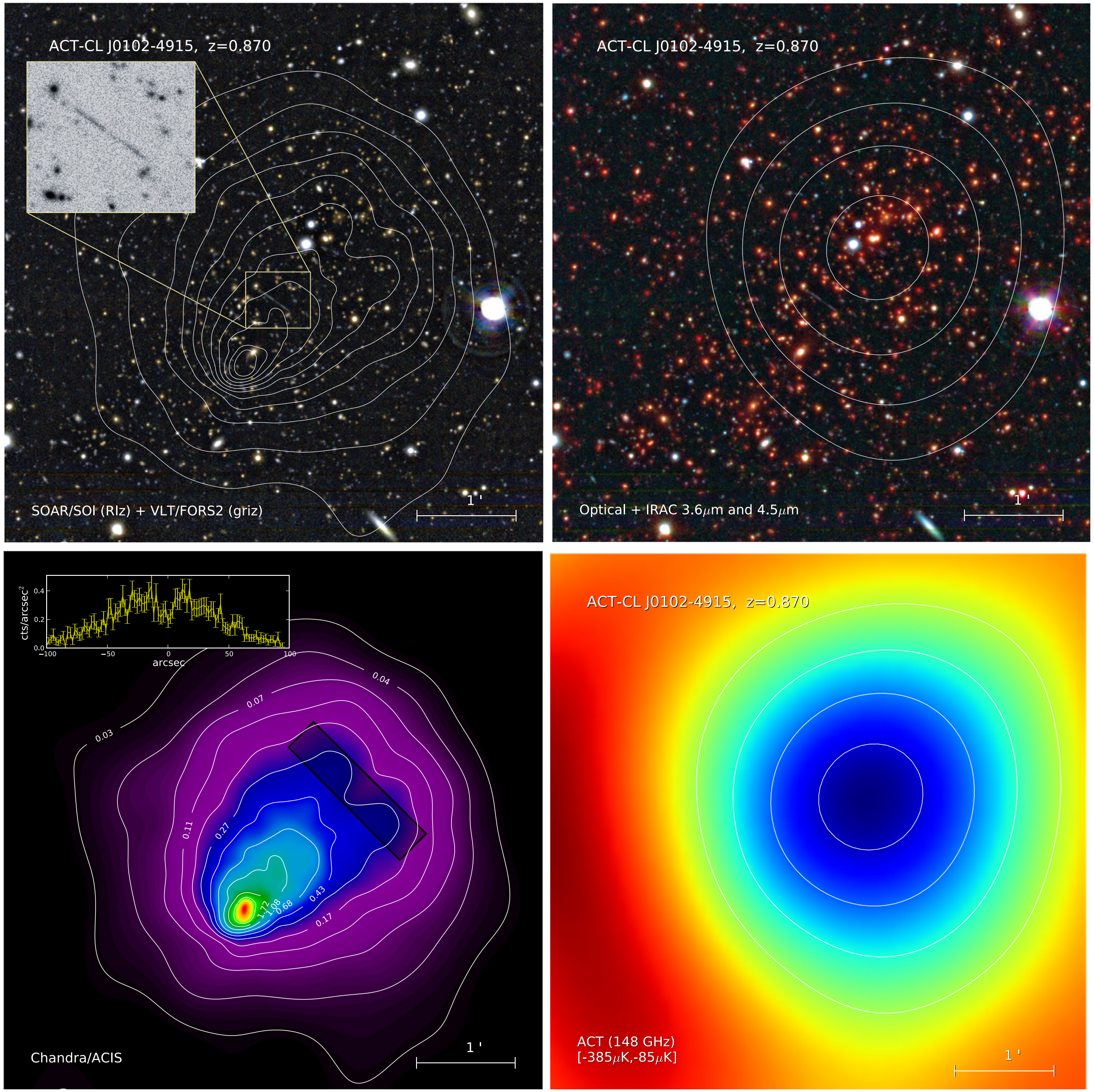

El Gordo !
The obese galaxy cluster

Figure 1. Multi-wavelength data set for ACT-CL J0102−4915 with all panels showing the same sky region. Upper left: the composite optical color image from the combined $griz$ (SOAR/SOI) and Riz (VLT/FORS2) imaging with the overplotted *Chandra* X-ray surface brightness contours shown in white. The black and white inset image shows a remarkably strong lensing arc. Upper right: the composite color image from the combination of the optical imaging from VLT and SOAR and IR from the *Spitzer*/IRAC 3.6 μm and 4.5 μm imaging. The overplotted linearly spaced contours in white correspond to the matched-filtered ACT 148 GHz intensity maps. Bottom left: false color image of the *Chandra* X-ray emission with the same set of 11 log-spaced contours between 2.71 counts arcsec^{-2} and 0.03 counts arcsec^{-2} as in the panel above. The inset here shows the X-ray surface brightness in a cut across the "wake" region from the box region shown. Bottom right: ACT 148 GHz intensity map with angular resolution of 1$'$.4 and match-filtered with a nominal galaxy cluster profile, in units of effective temperature difference from the mean. The color scale ranges from −85 μK at the edges to −385 μK at the center of the SZ minimum. In all panels the horizontal bar shows the scale of the image, where north is up and east is left.

Planck Early Results XXVI: Detection with *Planck* and confirmation by *XMM-Newton* of PLCK G266.6−27.3, an exceptionally X-ray luminous and massive galaxy cluster at $z \sim 1$

Planck Collaboration: N. Aghanim[50], M. Arnaud[64]⋆, M. Ashdown[62,4], F. Atrio-Barandela[14], J. Aumont[50], C. Baccigalupi[73], A. Balbi[31], A. J. Banday[82,7,68], R. B. Barreiro[58], J. G. Bartlett[3,60], E. Battaner[84], K. Benabed[51,80], A. Benoît[49], J.-P. Bernard[82,7], M. Bersanelli[28,44], R. Bhatia[5], H. Böhringer[69], A. Bonaldi[40], J. R. Bond[6], S. Borgani[29,42], J. Borrill[67,76], F. R. Bouchet[51,80], M. L. Brown[4,62], C. Burigana[43], P. Cabella[31], C. M. Cantalupo[67], B. Cappellini[44], P. Carvalho[4], A. Catalano[3,63], L. Cayón[22], L.-Y Chiang[54], C. Chiang[21], G. Chon[69,4], P. R. Christensen[70,32], E. Churazov[68,75], D. L. Clements[47], S. Colafrancesco[41], S. Colombi[51,80], B. P. Crill[60,71], F. Cuttaia[43], A. Da Silva[10], H. Dahle[56,9], L. Danese[73], O. D'Arcangelo[59], R. J. Davis[61], P. de Bernardis[27], G. de Gasperis[31], G. de Zotti[40,73], J. Delabrouille[3], J.-M. Delouis[51,80], J. Démoclès[64], F.-X. Désert[45], C. Dickinson[61], J. M. Diego[58], H. Dole[50], S. Donzelli[44,56], O. Doré[60,8], M. Douspis[50], X. Dupac[36], G. Efstathiou[55], T. A. Enßlin[68], H. K. Eriksen[56], F. Finelli[43], I. Flores-Cacho[57,33], O. Forni[82,7], P. Fosalba[52], M. Frailis[42], E. Franceschi[43], S. Fromenteau[3,50], S. Galeotta[42], K. Ganga[3,48], R. T. Génova-Santos[57,33], M. Giard[82,7], J. González-Nuevo[73], R. González-Riestra[35], K. M. Górski[60,85], A. Gregorio[29], A. Gruppuso[43], F. K. Hansen[56], D. Harrison[55,62], P. Heinämäki[79], C. Hernández-Monteagudo[68,11], S. R. Hildebrandt[8,65,57], E. Hivon[51,80], M. Hobson[4], G. Hurier[65], A. H. Jaffe[47], W. C. Jones[21], M. Juvela[20], E. Keihänen[20], R. Keskitalo[60,20], T. S. Kisner[67], R. Kneissl[34,5], H. Kurki-Suonio[20,39], G. Lagache[50], A. Lähteenmäki[1,39], J.-M. Lamarre[63], A. Lasenby[4,62], C. R. Lawrence[60], M. Le Jeune[3], S. Leach[73], R. Leonardi[36], C. Leroy[50,82,7], A. Liddle[19], P. B. Lilje[56,9], M. López-Caniego[58], G. Luzzi[66], J. F. Macías-Pérez[65], D. Maino[28,44], N. Mandolesi[43], F. Marleau[16], E. Martínez-González[58], S. Masi[27], S. Matarrese[26], P. Mazzotta[31], P. R. Meinhold[24], A. Melchiorri[27], J.-B. Melin[12], L. Mendes[36], A. Mennella[28,42], M.-A. Miville-Deschênes[50,6], A. Moneti[51,80], L. Montier[82,7], G. Morgante[43], D. Mortlock[47], D. Munshi[74,55], P. Naselsky[70,32], P. Natoli[30,2,43], J. Nevalainen[20,38], H. U. Nørgaard-Nielsen[13], F. Noviello[50], D. Novikov[47], I. Novikov[70], I. J. O'Dwyer[60], S. Osborne[77], R. Paladini[48], F. Pasian[42], G. Patanchon[3], T. J. Pearson[8,48], O. Perdereau[66], L. Perotto[65], F. Perrotta[73], F. Piacentini[27], E. Pierpaoli[18], R. Piffaretti[64,12], P. Platania[59], E. Pointecouteau[82,7], G. Polenta[2,41], N. Ponthieu[50], L. Popa[53], T. Poutanen[39,20,1], G. W. Pratt[64], G. Prézeau[8,60], S. Prunet[51,80], J.-L. Puget[50], J. P. Rachen[68], R. Rebolo[57,33], M. Reinecke[68], C. Renault[65], S. Ricciardi[43], T. Riller[68], I. Ristorcelli[82,7], G. Rocha[60,8], J. A. Rubiño-Martín[57,33], E. Saar[78], M. Sandri[43], G. Savini[72], B. M. Schaefer[81], D. Scott[17], G. F. Smoot[23,67,3], J.-L. Starck[64,12], D. Sutton[55,62], J.-F. Sygnet[51,80], J. A. Tauber[37], L. Terenzi[43], L. Toffolatti[15], M. Tomasi[28,44], M. Tristram[66], M. Türler[46], L. Valenziano[43], P. Vielva[58], F. Villa[43], N. Vittorio[31], L. A. Wade[60], B. D. Wandelt[51,80,25], J. Weller[83], S. D. M. White[68], M. White[23], D. Yvon[12], A. Zacchei[42], and A. Zonca[24]

(Affiliations can be found after the references)

Received June 7; Accepted July 11

Planck SZ clusters

ABSTRACT

We present first results on PLCK G266.6−27.3, a galaxy cluster candidate detected at a signal-to-noise ratio of 5 in the *Planck* All Sky survey. An *XMM-Newton* validation observation has allowed us to confirm that the candidate is a *bona fide* galaxy cluster. With these X-ray data we measure an accurate redshift, $z = 0.94 \pm 0.02$, and estimate the cluster mass to be $M_{500} = (7.8 \pm 0.8) \times 10^{14}\ \mathrm{M}_{\odot}$. PLCK G266.6−27.3 is an exceptional system: its luminosity of $L_X[0.5\text{–}2.0\mathrm{keV}] = (1.4 \pm 0.05) \times 10^{45}\ \mathrm{erg\ s^{-1}}$ equals that of the two most luminous known clusters in the $z > 0.5$ universe, and it is one of the most massive clusters at $z \sim 1$. Moreover, unlike the majority of high-redshift clusters, PLCK G266.6−27.3 appears to be highly relaxed. This observation confirms *Planck*'s capability of detecting high-redshift, high-mass clusters, and opens the way to the systematic study of population evolution in the exponential tail of the mass function.

Key words. Cosmology: observations – Galaxies: cluster: general – Galaxies: clusters: intracluster medium – Cosmic background radiation, X-rays: galaxies: clusters

Monthly Notices of the ROYAL ASTRONOMICAL SOCIETY

MNRAS **439,** 48–72 (2014) doi:10.1093/mnras/stt2129
Advance Access publication 2014 February 4

Weighing the Giants – III. Methods and measurements of accurate galaxy cluster weak-lensing masses

Douglas E. Applegate,[1,2,3,4]★ Anja von der Linden,[1,2,5] Patrick L. Kelly,[1,2,3] Mark T. Allen,[1,2] Steven W. Allen,[1,2,3] Patricia R. Burchat,[1,2] David L. Burke,[1,3] Harald Ebeling,[6] Adam Mantz[7,8] and R. Glenn Morris[1,3]

[1] *Kavli Institute for Particle Astrophysics and Cosmology, Stanford University, 452 Lomita Mall, Stanford, CA 94305-4085, USA*
[2] *Department of Physics, Stanford University, 382 Via Pueblo Mall, Stanford, CA 94305-4060, USA*
[3] *SLAC National Accelerator Laboratory, 2575 Sand Hill Road, Menlo Park, CA 94025, USA*
[4] *Argelander-Institut für Astronomie, Universität Bonn, Auf dem Hügel 71, D-53121 Bonn, Germany*
[5] *Dark Cosmology Centre, Niels Bohr Institute, University of Copenhagen, Juliane Maries Vej 30, DK-2100 Copenhagen, Denmark*
[6] *Institute for Astronomy, 2680 Woodlawn Drive, Honolulu, HI 96822, USA*
[7] *Kavli Institute for Cosmological Physics, University of Chicago, 5640 South Ellis Avenue, Chicago, IL 60637-1433, USA*
[8] *Department of Astronomy and Astrophysics, University of Chicago, 5640 South Ellis Avenue, Chicago, IL 60637-1433, USA*

Accepted 2013 November 4. Received 2013 October 7; in original form 2012 August 1

ABSTRACT

We report weak-lensing masses for 51 of the most X-ray luminous galaxy clusters known. This cluster sample, introduced earlier in this series of papers, spans redshifts $0.15 \lesssim z_{\rm cl} \lesssim 0.7$, and is well suited to calibrate mass proxies for current cluster cosmology experiments. Cluster masses are measured with a standard 'colour-cut' lensing method from three-filter photometry of each field. Additionally, for 27 cluster fields with at least five-filter photometry, we measure high-accuracy masses using a new method that exploits all information available in the photometric redshift posterior probability distributions of individual galaxies. Using simulations based on the COSMOS-30 catalogue, we demonstrate control of systematic biases in the mean mass of the sample with this method, from photometric redshift biases and associated uncertainties, to better than 3 per cent. In contrast, we show that the use of single-point estimators in place of the full photometric redshift posterior distributions can lead to significant redshift-dependent biases on cluster masses. The performance of our new photometric redshift-based method allows us to calibrate 'colour-cut' masses for all 51 clusters in the present sample to a total systematic uncertainty of ≈7 per cent on the mean mass, a level sufficient to significantly improve current cosmology constraints from galaxy clusters. Our results bode well for future cosmological studies of clusters, potentially reducing the need for exhaustive spectroscopic calibration surveys as compared to other techniques, when deep, multifilter optical and near-IR imaging surveys are coupled with robust photometric redshift methods.

Key words: gravitational lensing: weak – methods: data analysis – methods: statistical – galaxies: clusters: general – galaxies: distances and redshifts – cosmology: observations.

1 INTRODUCTION

Galaxy clusters have become a cornerstone of the experimental evidence supporting the standard ΛCDM cosmological model. Recent studies of statistical samples of clusters have placed precise and robust constraints on fundamental parameters, including the amplitude of the matter power spectrum, the dark energy equation of state and departures from General Relativity on large scales. For a review of recent progress and future prospects, see Allen, Evrard & Mantz (2011).

Typical galaxy cluster number count experiments require a mass-observable scaling relation to infer cluster masses from survey data, which in turn requires calibration of the mass-proxy bias and scatter. Weak lensing follow-up of clusters can be used, and to some extent has already been used, to set the absolute calibrations for the mass–observable relations employed in current X-ray and optical cluster count surveys (e.g. Mantz et al. 2008, 2010a; Vikhlinin et al. 2009b; Rozo et al. 2010). However, targeted weak lensing

Table 4 – *continued*

Cluster	Redshift	$P(z)$ method r_s (Mpc)	$P(z)$ method $M(<1.5\,{\rm Mpc})$ ($10^{14}\,{\rm M_\odot}$)	Color-cut method r_s (Mpc)	Color-cut method $M(<1.5\,{\rm Mpc})$ ($10^{14}\,{\rm M_\odot}$)
(1)	(2)	(3)	(4)	(5)	(6)
MS0451.6−0305	0.538	$0.39^{+0.15}_{-0.11}$	$8.8^{+3.3}_{-3.2}$	$0.49^{+0.06}_{-0.07}$	$12.5^{+3.5}_{-3.7}$
MACSJ1423.8+2404	0.543	$0.25^{+0.11}_{-0.11}$	$3.7^{+2.8}_{-2.2}$	$0.42^{+0.07}_{-0.09}$	$8.8^{+3.6}_{-3.6}$
MACSJ1149.5+2223	0.544	$0.49^{+0.18}_{-0.13}$	$14.4^{+3.3}_{-3.3}$	$0.51^{+0.05}_{-0.06}$	$13.6^{+3.1}_{-3.1}$
MACSJ0717.5+3745	0.546	$0.68^{+0.27}_{-0.18}$	$25.3^{+4.1}_{-4.2}$	$0.66^{+0.05}_{-0.06}$	$23.1^{+3.7}_{-3.8}$
016+16	0.547	$0.54^{+0.18}_{-0.15}$	$15.0^{+3.7}_{-3.6}$	$0.58^{+0.05}_{-0.05}$	$17.5^{+3.2}_{-3.1}$
CSJ0025.4−1222	0.585	$0.41^{+0.14}_{-0.13}$	$11.5^{+3.0}_{-3.1}$	$0.48^{+0.05}_{-0.06}$	$12.3^{+2.9}_{-2.9}$
CSJ2129.4−0741	0.588	–	–	$0.52^{+0.05}_{-0.05}$	$15.1^{+3.2}_{-3.1}$
CSJ0647.7+7015	0.592	$0.45^{+0.19}_{-0.14}$	$13.3^{+5.7}_{-5.6}$	$0.52^{+0.08}_{-0.10}$	$14.9^{+5.2}_{-5.3}$
CSJ0744.8+3927	0.698	$0.48^{+0.19}_{-0.12}$	$20.5^{+5.7}_{-5.7}$	$0.56^{+0.06}_{-0.06}$	$20.0^{+4.5}_{-4.4}$

Monthly Notices
of the
ROYAL ASTRONOMICAL SOCIETY

MNRAS **429,** 2910–2916 (2013) doi:10.1093/mnras/sts497

A structure in the early Universe at $z \sim 1.3$ that exceeds the homogeneity scale of the R-W concordance cosmology

Roger G. Clowes,[1★] Kathryn A. Harris,[1] Srinivasan Raghunathan,[1,2†] Luis E. Campusano,[2] Ilona K. Söchting[3] and Matthew J. Graham[4]

[1] *Jeremiah Horrocks Institute, University of Central Lancashire, Preston PR1 2HE*
[2] *Observatorio Astronómico Cerro Calán, Departamento de Astronomía, Universidad de Chile, Casilla 36-D, Santiago, Chile*
[3] *Astrophysics, Denys Wilkinson Building, Keble Road, University of Oxford, Oxford OX1 3RH*
[4] *California Institute of Technology, 1200 East California Boulevard, Pasadena, CA 91125, USA*

The Large Quasar Groups (LQGs)

Accepted 2012 November 24. Received 2012 November 12; in original form 2012 October 12

ABSTRACT

A large quasar group (LQG) of particularly large size and high membership has been identified in the DR7QSO catalogue of the Sloan Digital Sky Survey. It has characteristic size (volume$^{1/3}$) $\sim$500 Mpc (proper size, present epoch), longest dimension $\sim$1240 Mpc, membership of 73 quasars and mean redshift $\bar{z} = 1.27$. In terms of both size and membership, it is the most extreme LQG found in the DR7QSO catalogue for the redshift range $1.0 \le z \le 1.8$ of our current investigation. Its location on the sky is $\sim 8\overset{\circ}{.}8$ north ($\sim$615 Mpc projected) of the Clowes & Campusano LQG at the same redshift, $\bar{z} = 1.28$, which is itself one of the more extreme examples. Their boundaries approach to within $\sim 2^\circ$ ($\sim$140 Mpc projected). This new, Huge-LQG appears to be the largest structure currently known in the early Universe. Its size suggests incompatibility with the Yadav et al. scale of homogeneity for the concordance cosmology, and thus challenges the assumption of the cosmological principle.

Key words: galaxies: clusters: general – quasars: general – large-scale structure of Universe.

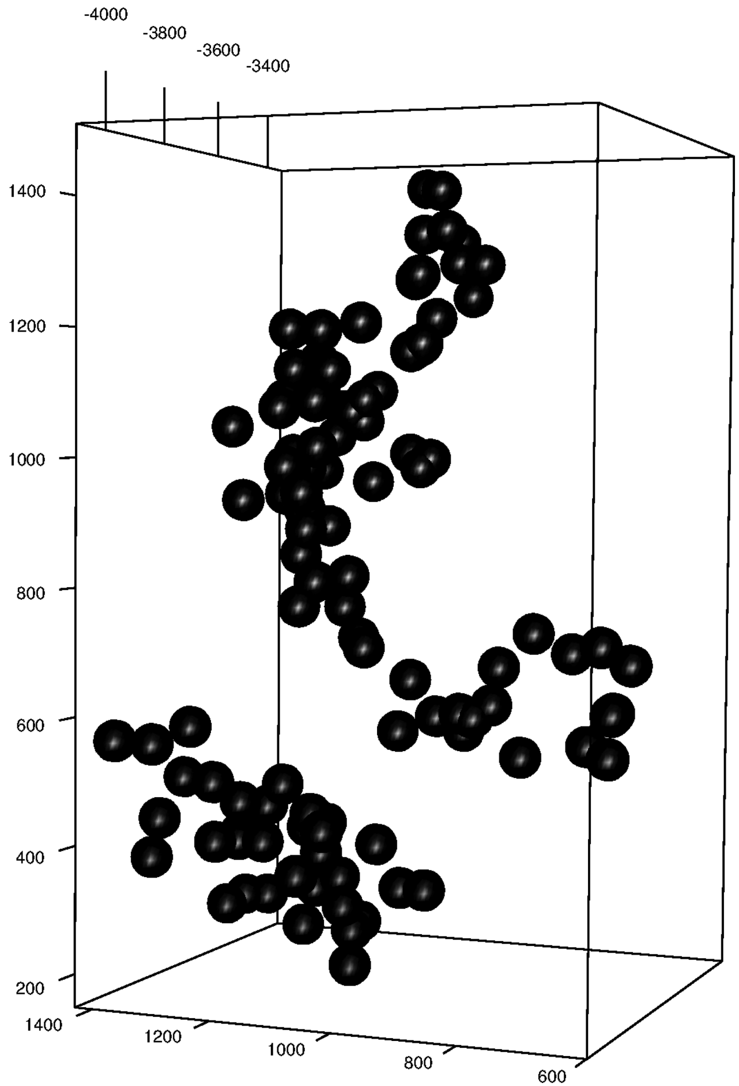

Figure 2. Snapshot from a visualization of both the new, Huge-LQG, and the CCLQG. The scales shown on the cuboid are proper sizes (Mpc) at the present epoch. The tick marks represent intervals of 200 Mpc. The Huge-LQG appears as the upper LQG. For comparison, the members of both are shown as spheres of radius 33.0 Mpc (half of the mean linkage for the Huge-LQG; the value for the CCLQG is 38.8 Mpc). For the Huge-LQG, note the dense, clumpy part followed by a change in orientation and a more filamentary part. The Huge-LQG and the CCLQG appear to be distinct entities.

The Large Quasar Groups (LQGs)

The temperature fluctuations of the cosmic microwave background (CMB)

- Initial seeds of present large scale structures
- Gaussian random field ?

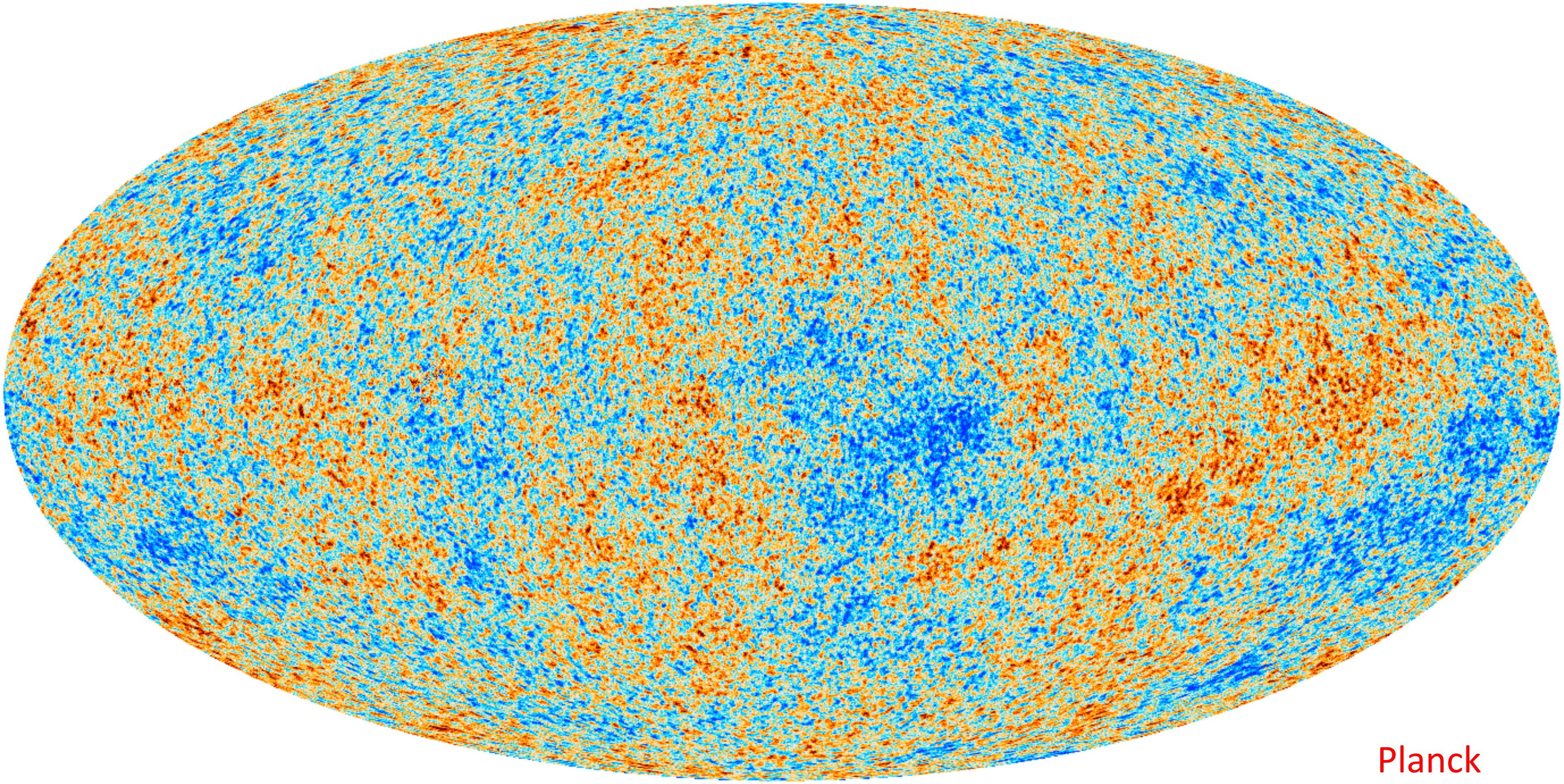

Planck

http://www.esa.int/Our_Activities/Space_Science/Planck

Mon. Not. R. Astron. Soc. **356,** 29–40 (2005) doi:10.1111/j.1365-2966.2004.08419.x

Detection of a non-Gaussian spot in *WMAP*

M. Cruz,[1,2]★ E. Martínez-González,[1] P. Vielva[3] and L. Cayón[4]

[1] *IFCA, CSIC-Univ. de Cantabria, Avda. los Castros, s/n, 39005-Santander, Spain*
[2] *Dpto. de Física Moderna, Univ. de Cantabria, Avda. los Castros, s/n, 39005-Santander, Spain*
[3] *Physique Corpusculaire et Cosmologie, Collège de France, 11 pl. M. Berthelot, F-75231 Paris Cedex 5, France*
[4] *Department of Physics, Purdue University, 525 Northwestern Avenue, West Lafayette, IN 47907-2036, USA*

Accepted 2004 September 20. Received 2004 July 26; in original form 2004 May 18

ABSTRACT

An extremely cold and big spot in the *Wilkinson Microwave Anisotropy Probe* (*WMAP*) 1-yr data is analysed. Our work is a continuation of a previous paper by Vielva et al. that reported the detection of non-Gaussianity, with a method based on the spherical Mexican hat wavelet (SMHW) technique. We study the spots at different thresholds on the SMHW coefficient maps, considering six estimators, namely the number of maxima, the number of minima, the numbers of hot and cold spots, and the number of pixels of those spots. At SMHW scales around 4° (10° on the sky), the data deviate from Gaussianity. The analysis is performed on all of the sky, the Northern and Southern hemispheres, and on four regions covering all of the sky. A cold spot at $(b = -57°, l = 209°)$ is found to be the source of this non-Gaussian signature. We compare the spots of our data with 10 000 Gaussian simulations, and conclude that only around 0.2 per cent of them present such a cold spot. Excluding this spot, the remaining map is compatible with Gaussianity, and even the excess of kurtosis in the paper by Vielva et al. is found to be due exclusively to this spot. Finally, we study whether the spot causing the observed deviation from Gaussianity could be generated by systematics or foregrounds. None of them seem to be responsible for the non-Gaussian detection.

Key words: methods: data analysis – cosmic microwave background.

The cold spot: an anomaly of physical origin or a simple statistical fluctuation ?

Cruz et al. 2005, MNRAS 356, 29

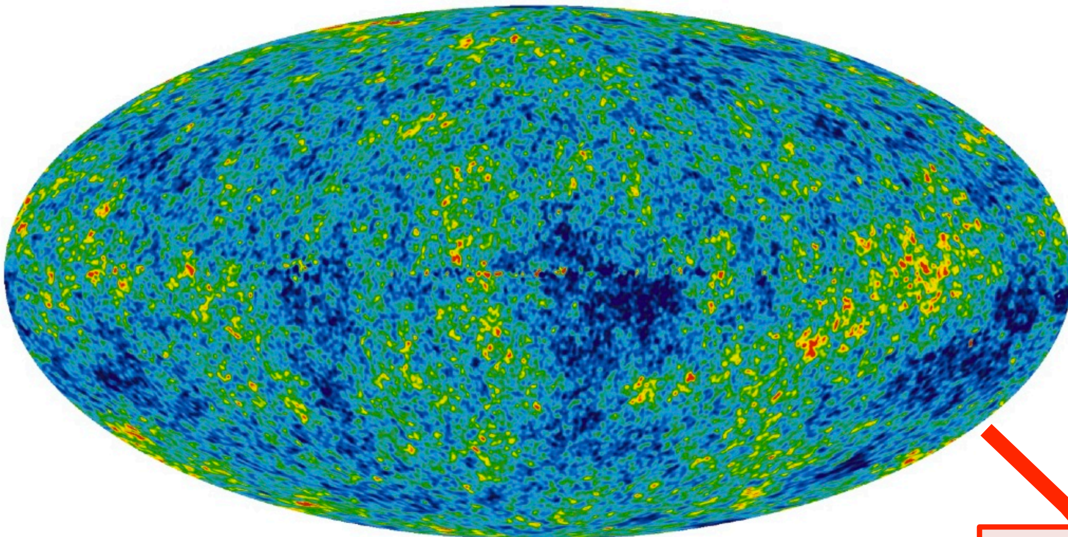

Spherical mexican hat wavelet transform

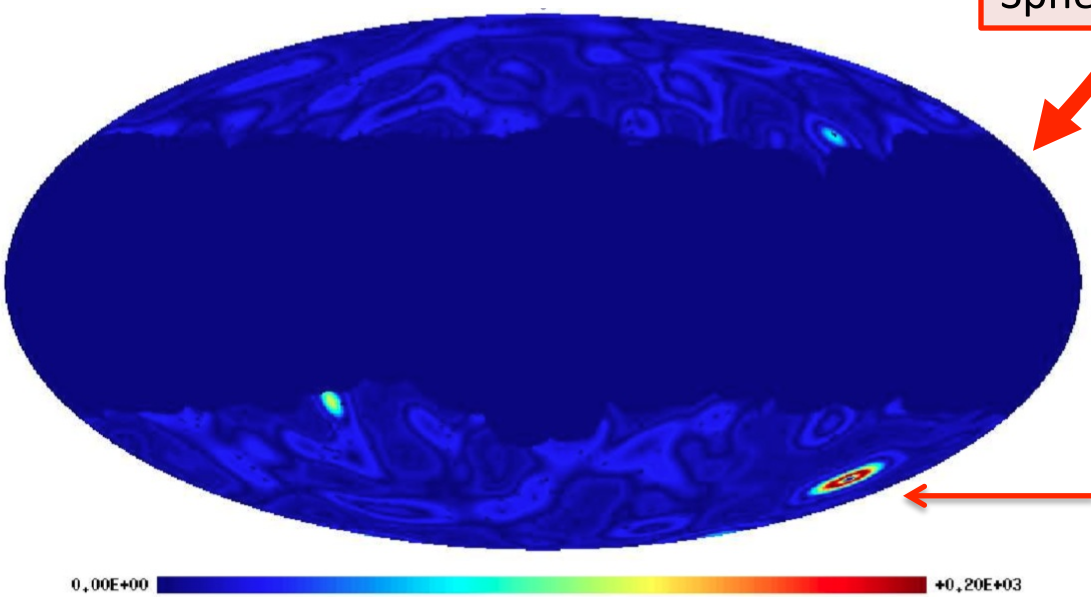

Cold spot

The Gumbel or extreme value statistics (EVS)

Gumbel 1958, Statistics of Extremes (2004, Dover)

Cumulative distribution of the maximum or minimum ν drawn from a finite patch in a random distribution.

It is often parameterized as follows

$$G_{\gamma_G}(\nu) = \exp[-(1+\gamma_G y)^{-1/\gamma_G}] \qquad y = \frac{\nu - a}{b}$$

a: location parameter
b: scale parameter
γ_G: shape parameter

$\gamma_G>0$: Fréchet type
$\gamma_G=0$: Gumbel type (expected asymptotically for Gaussian fields)

$$G_0 = \exp[-\exp(-y)]$$

$\gamma_G<0$: negative Weibull type

The properties of the extreme value statistics (EVS)

Equivalence of the Central Limit theorem:

For N random independent variables x_i $i=1,\ldots,N$ with the same law, the cumulative distribution of the random variable

$M_N = \max_i x_i$

necessarily tends asymptotically for large N to one of the 3 distributions of the previous slide (if such a limit exists).

(Fisher & Tippett 1928 Proc. Camb. Phil. Soc. 24, 180
Gnedenko 1943, Ann. of Math. 44, 423)

So the EVS is potentially at the same time interesting (specific statistical predictions for rare events) and uninteresting (everything lead to the same: poor constraining power)

Mon. Not. R. astr. Soc. (1985) **213,** 857–869

First ranked galaxies in groups and clusters

Suketu P. Bhavsar *Raman Research Institute, Bangalore 560080, India, and Astronomy Centre, University of Sussex, Brighton BN1 9QH*

John D. Barrow *Astronomy Centre, University of Sussex, Brighton BN1 9QH*

Accepted 1984 December 3. Received 1984 October 10

Summary. The small scatter in the luminosities of the brightest galaxies in clusters has been a topic of much debate. It has been argued that these galaxies are either special objects or the tail-end of a statistical distribution. In 1928, Fisher and Tippett derived the general form a distribution of extreme sample values should take, independent of the parent distribution from which they are drawn. We compare this asymptotic form with the distribution of first ranked cluster members and conclude that these galaxies are not the extreme members of a statistical population. On the other hand, comparison of first ranked members of 'loose' groups with the extreme value distributions shows that these galaxies are consistent with their being the tail-end of a statistical distribution.

Bhavsar and Barrow use both the
interesting
and the
uninteresting
(or conversely) aspects of the EVS !

Example 1: the most massive galaxy cluster

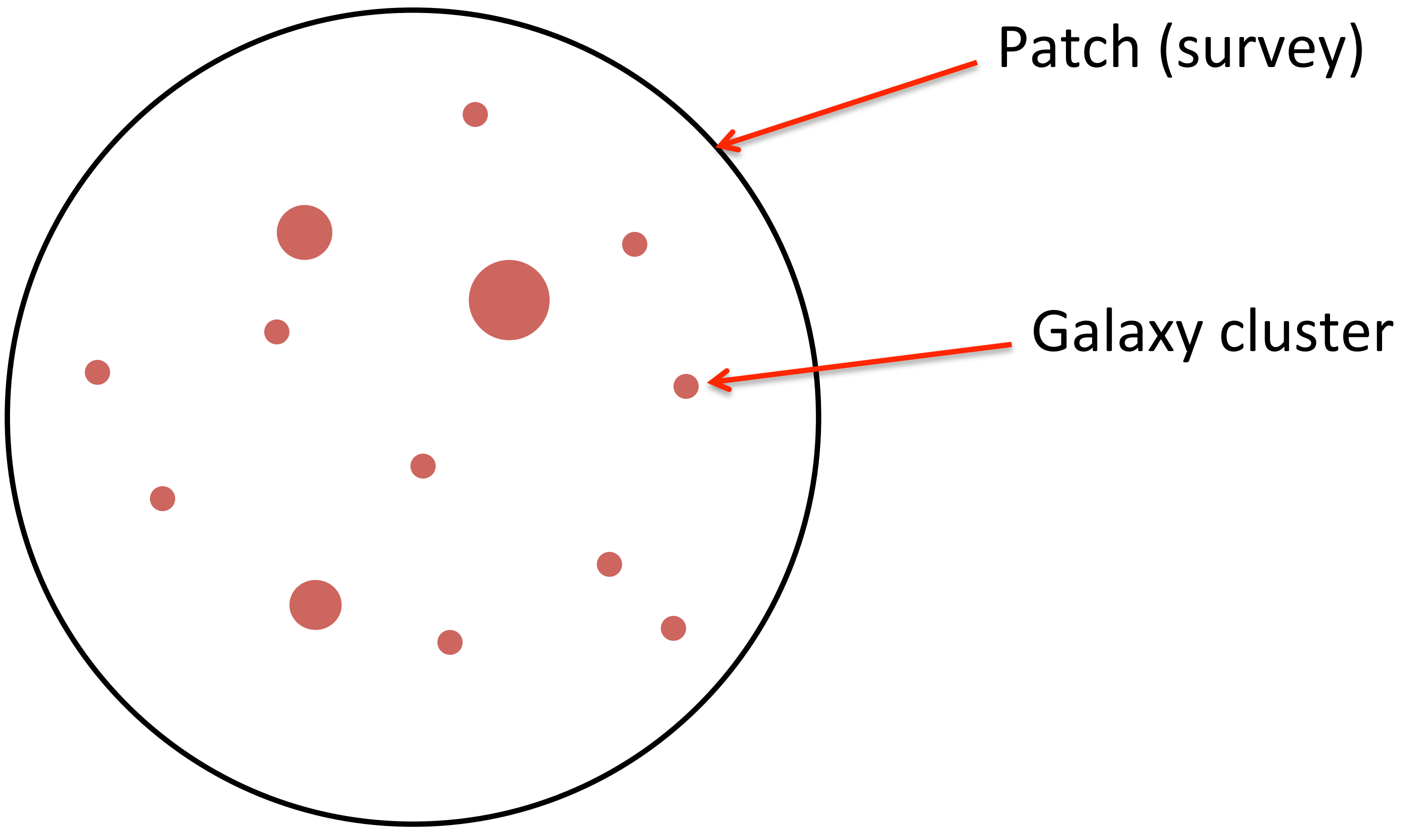

What is the typical mass M_{max} of the most massive cluster in the survey?
What is the probability $P_{evs}(M_{max} < M_{th})$ of having $M_{max} < M_{th}$?
What is the most massive cluster in the observable Universe?

The probability $P_{evs}(M_{max} < M_{th})$ is the probability that all the clusters in the survey have a mass smaller than M_{th}.

If the mass of a cluster is statistically independent from the mass of other clusters the naive result is simply

$$P_{evs}(M_{max} < M_{th})=[1-Q(M_{max} > M_{th})]^N$$

where $Q(M > M_{th})$ is the probability that a cluster has a mass M larger than M_{th} and N is the number of clusters.

$$P(M_{max} < M_{th})=\exp[\, N \ln (1-Q(M > M_{th})]$$
$$\approx\exp[-N\, Q(M > M_{th})]$$

in the very massive cluster regime

Hence

$$P(M_{max} < M_{th}) \approx\exp[\, - n(M_{max} > M_{th})\, V]$$

Where $n(M_{max} > M_{th})$ is the number density of clusters with mass larger than M_{th} and V is the survey volume

Issues:

- Definition : what is a cluster of galaxies?

- How to compute $n(M_{max} > M_{th})$? Press & Schechter formalism and extensions: easy calculations (e.g. Davis et al. 2011; Holz & Perlmutter 2012; Harrison & Coles, 2012; Waizman et al. 2012, 2013), even including the possible non Gaussian nature of the initial seeds (e.g. Cayón, Gordon & Silk 2011, MNRAS 415, 849)

- Clusters are correlated: the correlations can be taken into account by reducing the EVS to a void probability (see cumbersome slides later): however, correlations should be negligible for large surveys (Davis et al. 2011, MNRAS 413, 2087)

- Tests of theoretical predictions : need ultragigabig simulations

- Negative Weibull favored (Υ_G=-0.21) when fitting the expected analytic form (Davis et al. 2011)

The HORIZON 4Π dark matter simulation performed with RAMSES on Platine at CEA, 4096^3 particles in a cube $2000h^{-1}$ Mpc aside. Teyssier et al. 2009, A&A 497, 335

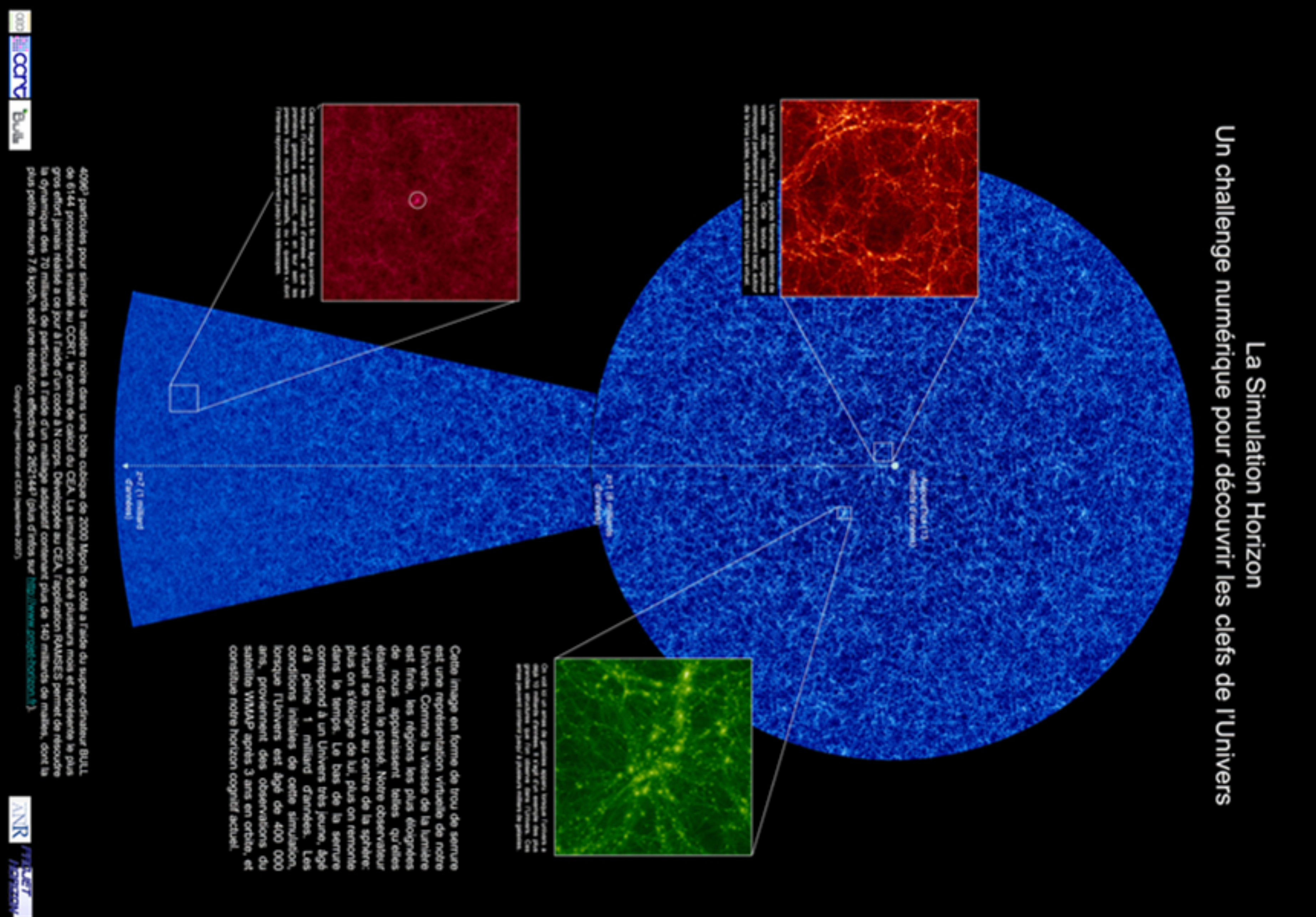

The probability distribution function of the most massive cluster

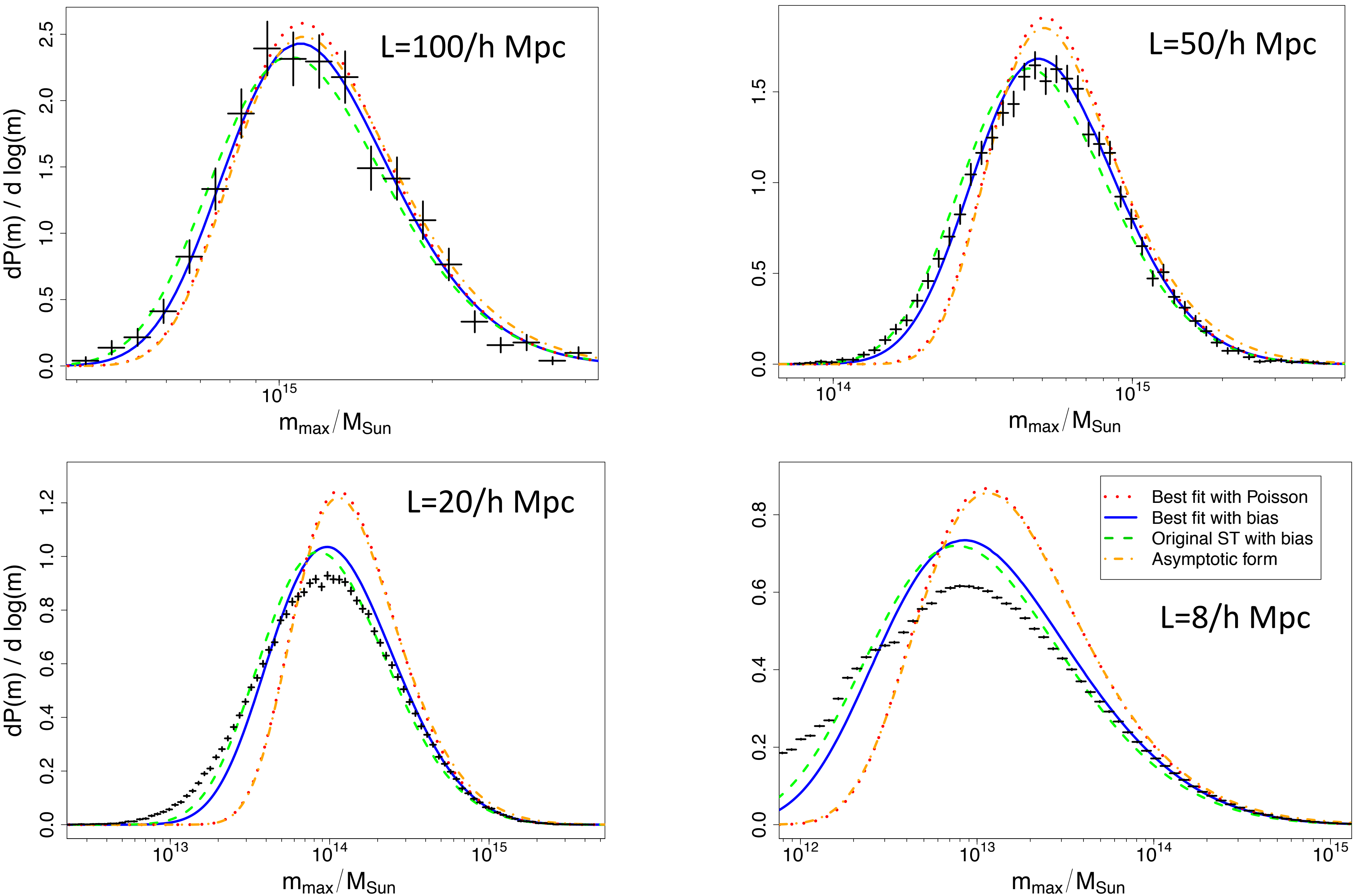

The most likely mass of the most massive cluster as a function of survey size

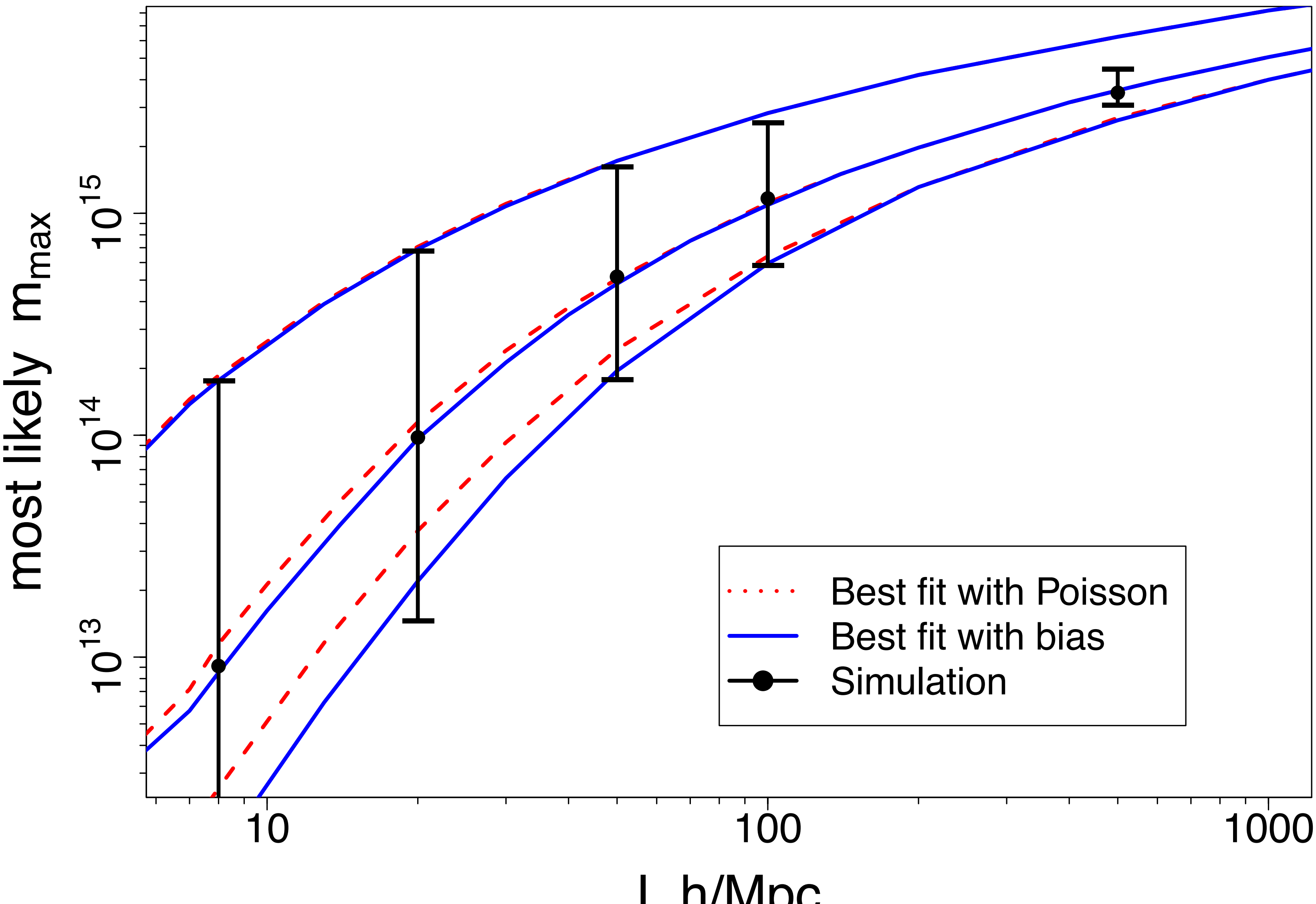

Application to observational data (a)

The Astrophysical Journal Letters, 755:L36 (4pp), 2012 August 20 doi:10.1088/2041-8205/755/2/L36

THE MOST MASSIVE OBJECTS IN THE UNIVERSE

Daniel E. Holz[1] and Saul Perlmutter[2,3]
[1] Enrico Fermi Institute, Department of Physics, and Kavli Institute for Cosmological Physics, University of Chicago, Chicago, IL 60637, USA
[2] Department of Physics, University of California Berkeley, Berkeley, CA 94720-7300, USA
[3] Lawrence Berkeley National Laboratory, Berkeley, CA 94720, USA
Received 2011 February 22; accepted 2012 July 16; published 2012 August 7

ABSTRACT

We calculate the expected mass of the most massive object in the universe, finding it to be a cluster of galaxies with total mass $M_{200} = 3.8 \times 10^{15} M_\odot$ at $z = 0.22$, with the 1σ marginalized regions being $3.3 \times 10^{15} M_\odot < M_{200} < 4.4 \times 10^{15} M_\odot$ and $0.12 < z < 0.36$. We restrict ourselves to self-gravitating bound objects and base our results on halo mass functions derived from N-body simulations. The mass and redshift distribution of the largest objects in the universe are potentially interesting tests of ΛCDM, probing the initial conditions, non-Gaussianity, and the behavior of gravity on large scales. We discuss A2163 and A370 as candidates for the most massive cluster in the universe, although uncertainties in their masses preclude definitive comparisons with theory. We find that the three most massive clusters in the South Pole Telescope (SPT) 178 and 2500 deg^2 catalogs match predictions. Since the mass function evolves steeply with redshift, we also investigate the most unlikely clusters in the universe. We find that SPT-CL J2106–5844 is 2σ and XMMU J2235.3–2557 is 3σ inconsistent with ΛCDM, considering their respective redshifts and survey sizes. Our findings motivate further observations of the highest mass end of the mass function, particularly at $z > 1$, where a number of anomalously massive clusters have been discovered. Future surveys will explore larger volumes, and both the most massive object and the most unlikely object in the universe may be identified within the next decade.

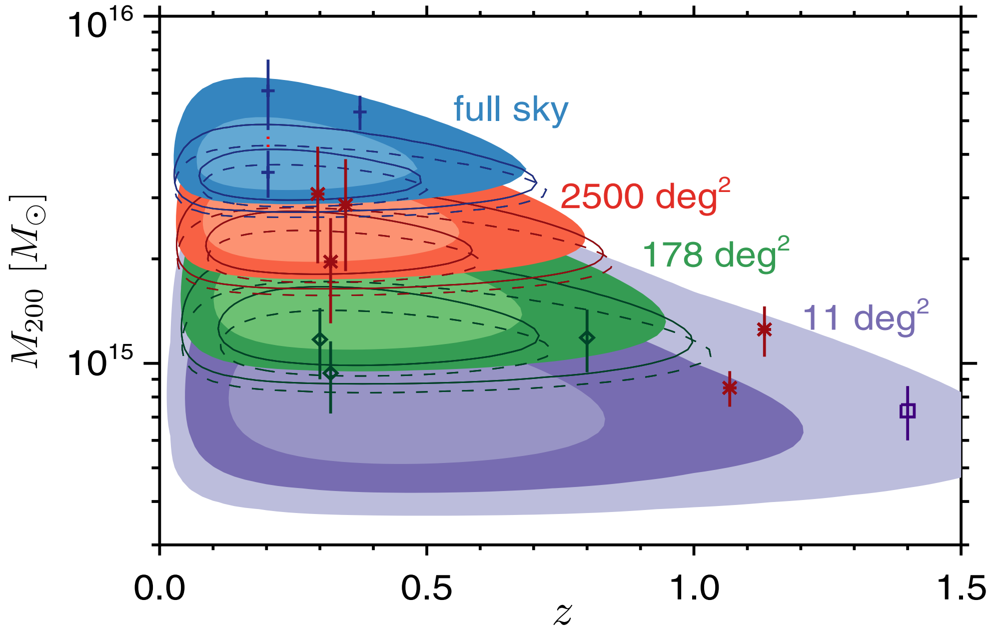

Figure 1. Contour plot of the most massive object in the universe. Four survey sizes are considered: full sky, 2500 and 178 deg^2 (corresponding to SPT), and 11 deg^2 (corresponding to XMM-2235). The shaded contours represent the 1σ and 2σ (and for the 11 deg^2 case, 3σ) regions of the most massive halo in a ΛCDM universe. 68% of all ΛCDM universes will have their most massive halo within the light blue 1σ contour. The pairs of solid line contours are 1σ and 2σ contours for the second most massive halo, while the pairs of dashed line contours are for the third most massive. The (blue) plus signs are A2163 (double point) and A370; the five (red) asterisks are the three most massive clusters from the SPT 2500 deg^2 survey and SPT-J2106 and SPT-J0546, two unusually massive clusters at $z > 1$; the three (green) diamonds are the three most massive clusters in the SPT 178 deg^2 survey; and the (purple) square is XMM-2235. The mass values for A2163 span the predicted region, while A370 is slightly high. The SPT masses fit within their respective contours, although SPT-J2106 is somewhat anomalous (with a probability of $\sim$0.06), and XMM-2235 is well outside its 2σ contour (with a probability of $\sim$0.006). All masses are M_{200} (spherical overdensity of 200× the background density); for data measured using different overdensities, we plot the M_{200} value which gives the equivalent probability.

Application to observational data (b)

Harrison & Coles, 2012, MNRAS 421, L19

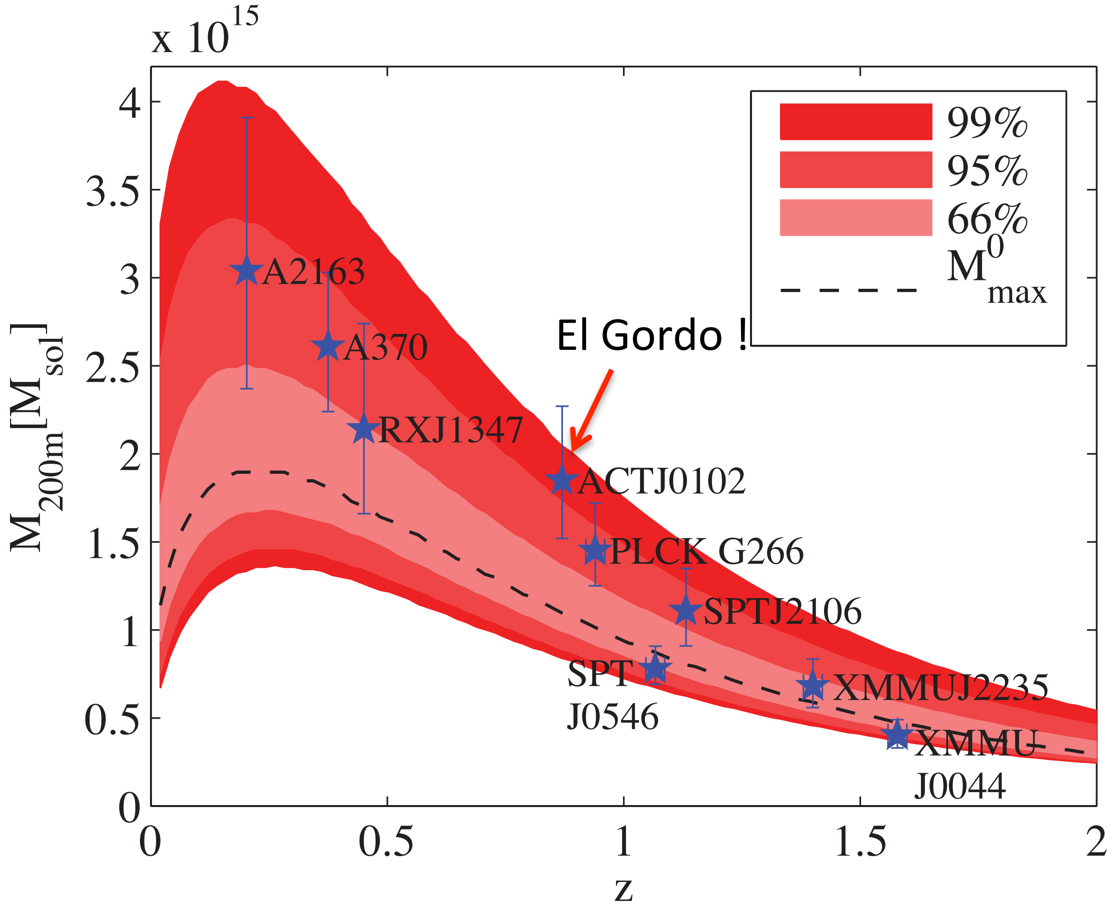

Figure 1. Extreme value contours and modal highest mass cluster with redshift for a ΛCDM cosmology, along with a set of currently observed 'extreme' galaxy clusters. None lies in the region above the 99 per cent contour and hence are consistent with a concordance cosmology.

Example 2: the maximum in a patch for a random field

What is the expected minimum (maximum) temperature of the CMB in a patch of the sky?

What is the expected temperature of the (hottest) coldest cold spot in the whole sky CMB?

(question first asked by Coles 1988, MNRAS 231, 125; **Colombi et al. 2011**)

Issues:
- Instrumental noise
- Contamination by foregrounds (non primordial sources, e.g. our Galaxy)
- The Gaussian nature of the fluctuations

The case of a smooth (Gaussian) random field

Colombi, Davis, Devriendt, Prunet & Silk, 2011, MNRAS 414, 2436

ν : Gaussian random field, stationary, isotropic, of zero average, smoothed with a window of size ℓ

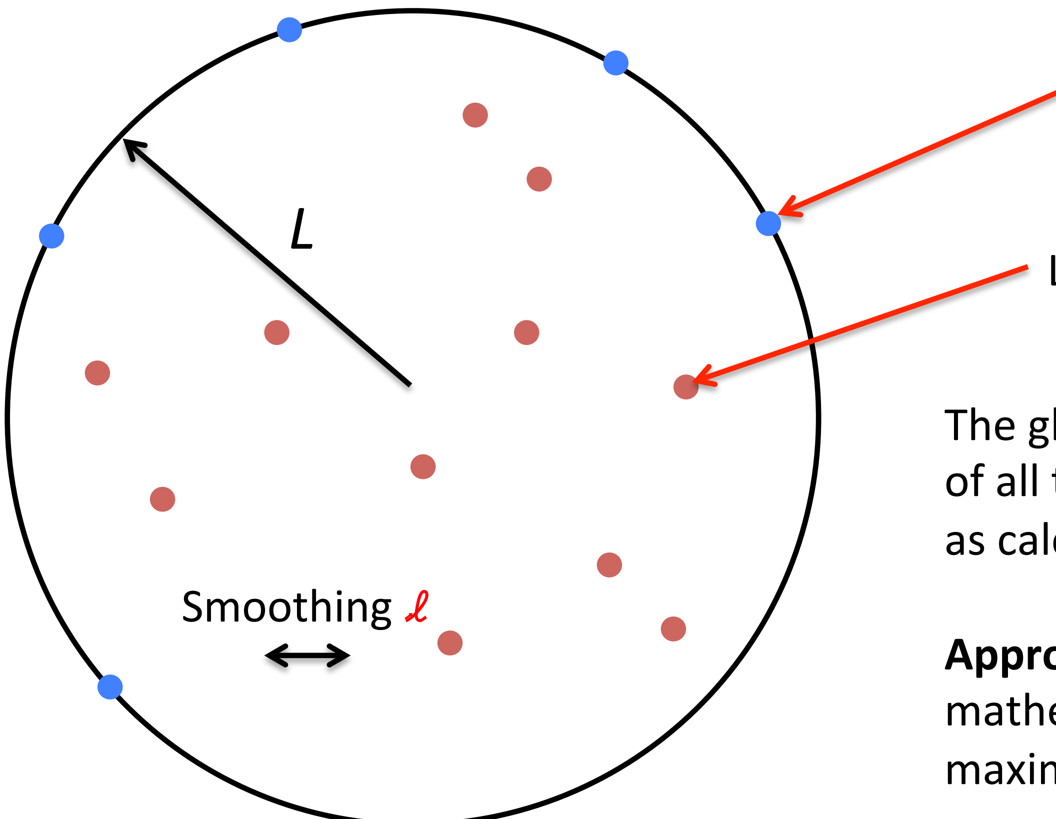

Local maximum along the edge: neglected

Local maximum inside the Patch

The global maximum is the maximum of all the local maxima including those as calculated on the edge:

Approximation : we (at variance with mathematicians) neglect the local maxima on the edges, i.e. the blue points. It should work if $L >> \ell$

What is the probability $P_{evs}(\nu_{max} < \nu_{th})$ of having $\nu_{max} < \nu_{th}$?
It can be reduced to the void probability $P_0(\nu_{th})$ of having no local maximum above the threshold ν_{th}

Extreme value statistics as a void probability

Generating function formalism (Balian & Schaeffer, 1989; Szapudi & Szalay 1993, ApJ 408, 43)

$$P_0(\nu_{\max}) = \exp\left[-nV\sigma(N_{\rm c})\right] \qquad \sigma(y) = \sum_{N\geq 1}(-1)^{N-1}\frac{S_N^{\rm p}}{N!}y^{N-1}$$

n: number density of peaks

V: volume of the patch $V = (4\pi/3)L^3$ $V = \pi L^2$

Deviation from pure Poisson: $N_{\rm c} \equiv nV\bar{\xi}_2^{\rm p}(L)$

Normalized cumulants: $S_N^{\rm p}(L) \equiv \dfrac{\bar{\xi}_N^{\rm p}(L)}{\bar{\xi}_2^{\rm p}(L)^{N-1}}, \quad S_1^{\rm p} \equiv S_2^{\rm p} \equiv 1$

Averaged reduced *N*-point correlations: $\bar{\xi}_N^{\rm p}(L) \equiv \dfrac{1}{V^N}\displaystyle\int_V {\rm d}^D x_1 \cdots {\rm d}^D x_N \xi_N^{\rm p}(x_1, \ldots, x_N)$

Approximation in the weak (but non zero) correlation limit

It can be shown, in the large threshold regime and in the weak correlation regime (Politzer & Wise 1984, ApJ 285, L1; Cline et al. 1987, CMaPh 112, 217)

$$\xi_N^{\mathrm{p}}(x_1,\ldots,x_N) \simeq \sum_{\text{trees}} \sum_{\text{labels}} \prod_{\text{links}} \xi_2^{\mathrm{p}}(x_i,x_j)$$

$$\nu \gg 1$$

$$\xi_2^{\mathrm{p}}(x_i,x_j) << 1$$

$N^{N\text{-}2}$ combinations

This is valid as well for a large variety of non Gaussian isotropic and stationary fields, e.g., obeying the general tree hierarchical model (Bernardeau & Schaeffer, 1999, A&A 349, 697)

$$S_N^{\mathrm{p}}(L) \simeq N^{N-2}$$

$$\sigma(y) = \left(1+\frac{1}{2}\theta\right)\mathrm{e}^{-\theta}, \quad \theta\mathrm{e}^{\theta} = y$$

Now we need just to compute the number density of peaks and their two-point correlation function, which can be easily performed, at least numerically, **using the theory of random Gaussian fields** (e.g., Adler 1981, The Geometry of Random fields).

We can use the calculations of Bardeen et al. (1986, ApJ 304, 15) in **3D** and Bond & Efstathiou (1987, MNRAS 226, 655) in **2D**

The Poisson limit (D=2 and 3)

Aldous 1989, Probability Approximations via the Poisson Clumping Heuristic

In the Poisson regime, N_c << 1, and for sufficiently large threshold, the extreme value statistics can be expressed as a function of the **Euler characteristic**

$P_{evs}(\nu)=$

$$P_{G,3}(\nu) \simeq \exp(-\mathcal{E}_3 V) = \exp\left[-U_3(\nu^2-1)\exp\left(-\frac{\nu^2}{2}\right)\right]$$

$$P_{G,2}(\nu) \simeq \exp(-\mathcal{E}_2 V) = \exp\left[-U_2\,\nu\exp\left(-\frac{\nu^2}{2}\right)\right]$$

$$U_D = \frac{\gamma^D V}{(2\pi)^{(D+1)/2} R_\star^D}$$

Note: $1 - P_{G,D}(\nu \gg 1) \simeq \mathcal{E}_D V$ (Adler, 1981; Adler & Taylor 2007, Random Fields and Geometry)

Coherence parameter: $\gamma \equiv \dfrac{\sigma_1^2}{\sigma_0\sigma_2}$

Scale length: $R_\star = \sqrt{D}\dfrac{\sigma_1}{\sigma_2}$

Moments of the power spectrum: $\sigma_j^2 \equiv \displaystyle\int \frac{k^{D-1}\mathrm{d}k}{2\pi^{D-1}} P(k) W_\ell^2(k) k^{2j}$

Scale free P(k) α k^n: $U_D = \left(\dfrac{4}{3}\right)^{D-2} \dfrac{\pi}{(2\pi)^{(D+1)/2}} \left(\dfrac{n+D}{2D}\right)^{D/2} \left(\dfrac{L}{\ell}\right)^D$

Link to the family of functions

$$G_{\gamma_G}(\nu) = \exp[-(1+\gamma_G y)^{-1/\gamma_G}] \qquad y = \frac{\nu - a}{b}$$

Taylor expansion around ν_* with $n(\nu_\star)V = 1$

$$\nu_\star \simeq \sqrt{2\ln U_D}\left[1 + \frac{(D-1)\ln(2\ln U_D)}{4\ln U_D}\right]$$

$$a = \nu_\star$$

$$b_3 = \frac{1}{\nu_\star}\frac{\nu_\star^2 - 1}{\nu_\star^2 - 3},$$

$$b_2 = \frac{\nu_\star}{\nu_\star^2 - 1},$$

$$U_D = \left(\frac{4}{3}\right)^{D-2} \frac{\pi}{(2\pi)^{(D+1)/2}} \left(\frac{n+D}{2D}\right)^{D/2} \left(\frac{L}{\ell}\right)^{D}$$

$$\gamma_{G,3} = -\frac{\nu_\star^4 + 3}{\nu_\star^2(\nu_\star^2 - 3)^2} < 0,$$

$$\gamma_{G,2} = -\frac{\nu_\star^2 + 1}{(\nu_\star^2 - 1)^2} < 0$$

One can therefore expect in practice negative Weibull because of the slow convergence of γ_G to zero.

Measurements in simulated 2D Gaussian fields

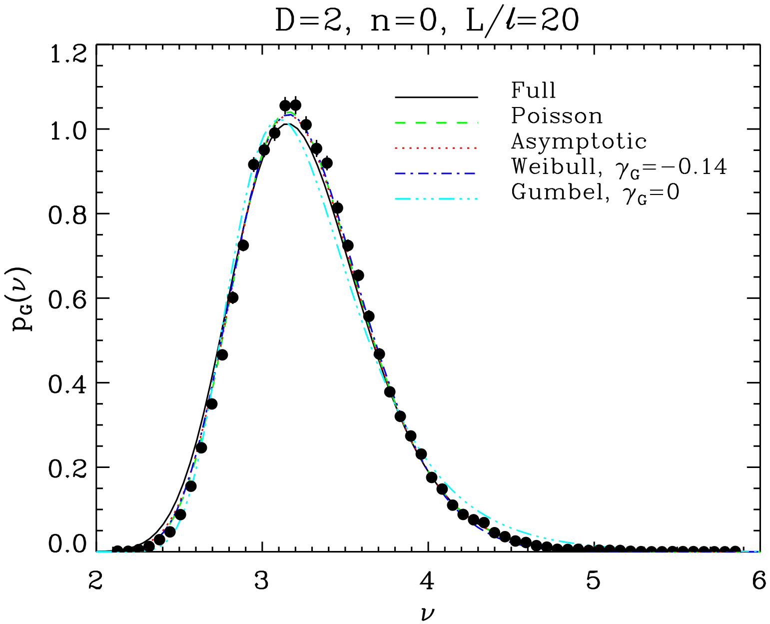

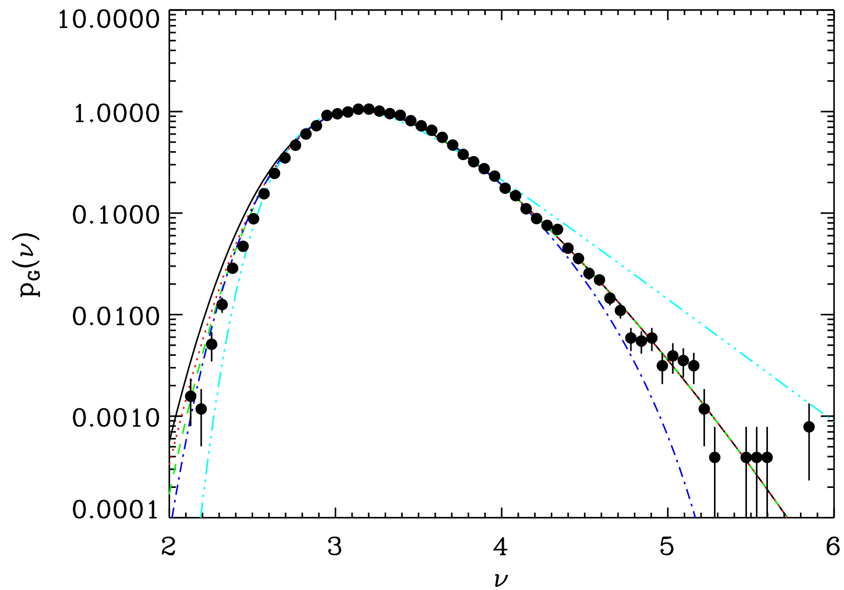

P(k) α k^n

100 realizations
4096^2 Pixels each
ℓ =5 pixels
400 non overlapping
patches of radius L=100
pixels per realization

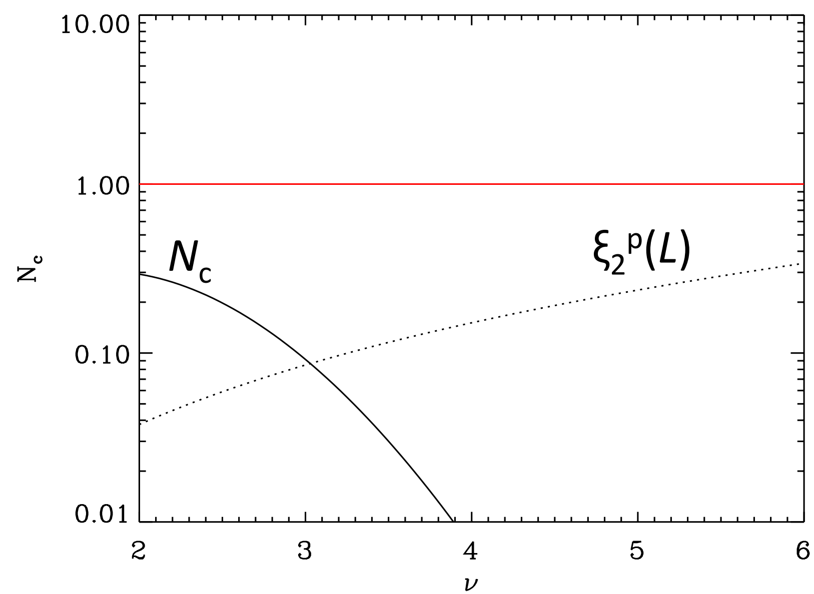

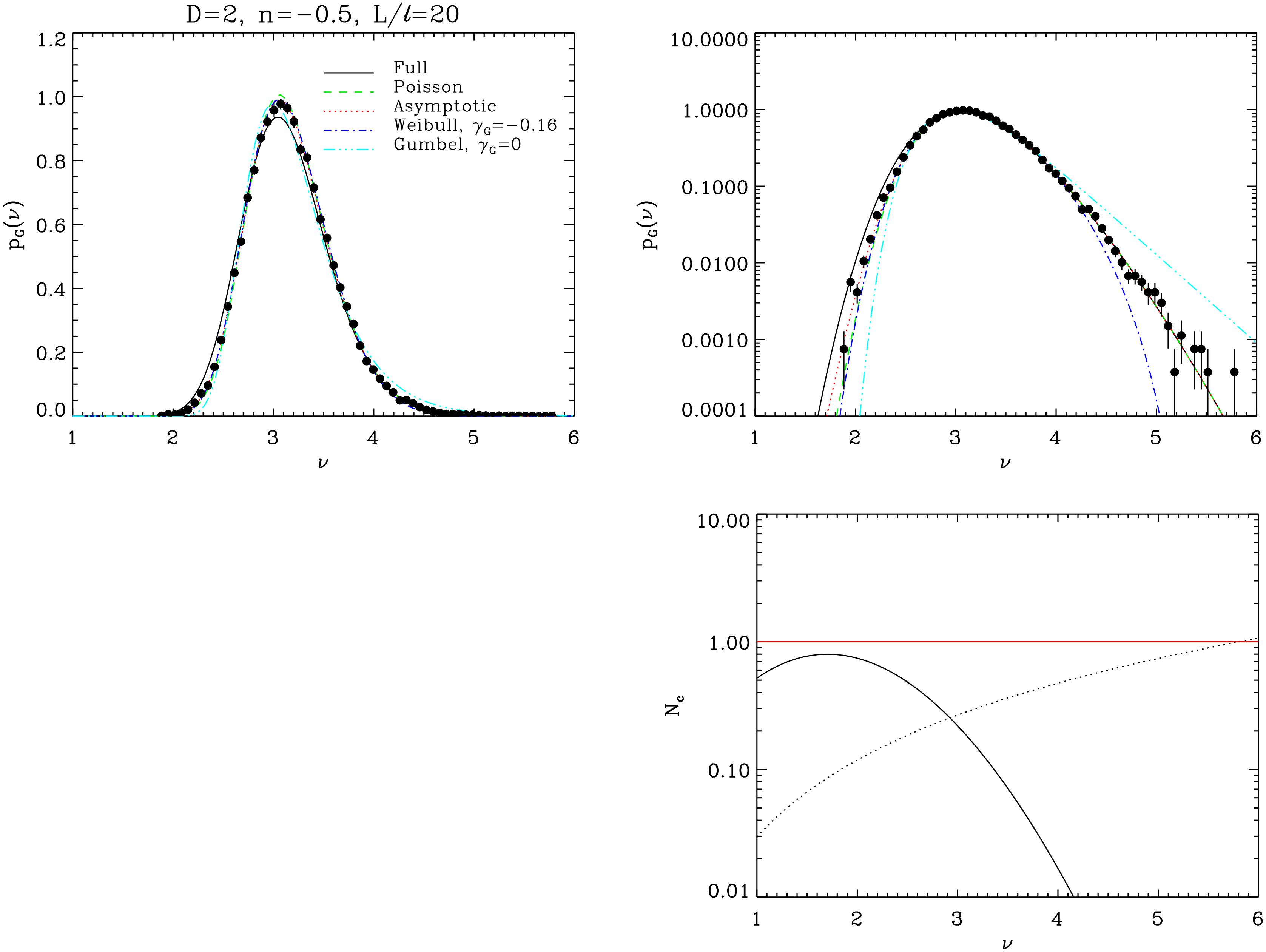

D=2, n=−0.5, L/ℓ=20
Full
Poisson
Asymptotic
Weibull, γG=−0.16
Gumbel, γG=0
pG(ν)
ν
Nc

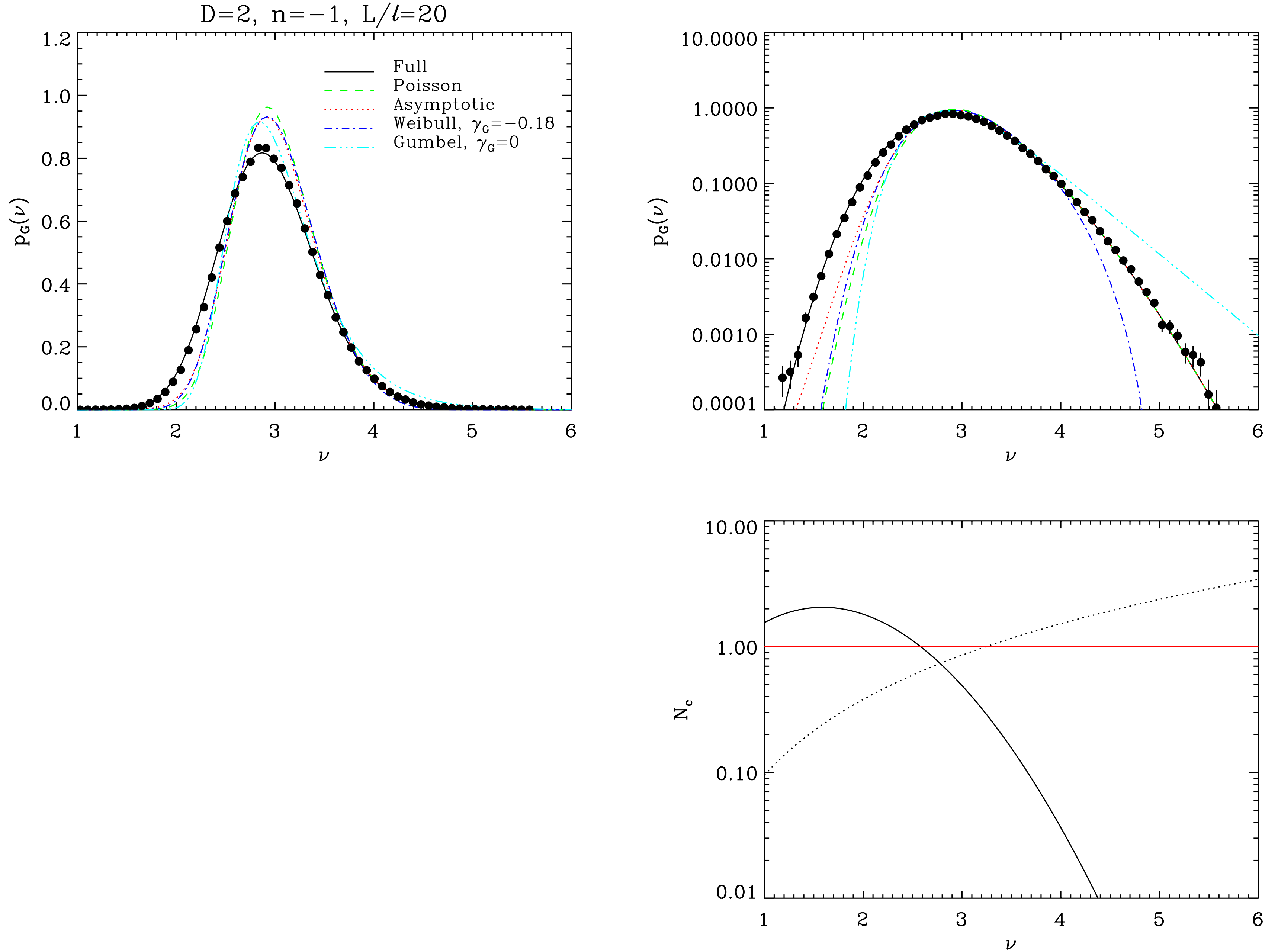
D=2, n=−1, L/ℓ=20
Full
Poisson
Asymptotic
Weibull, γG=−0.18
Gumbel, γG=0
pG(ν)
ν
Nc

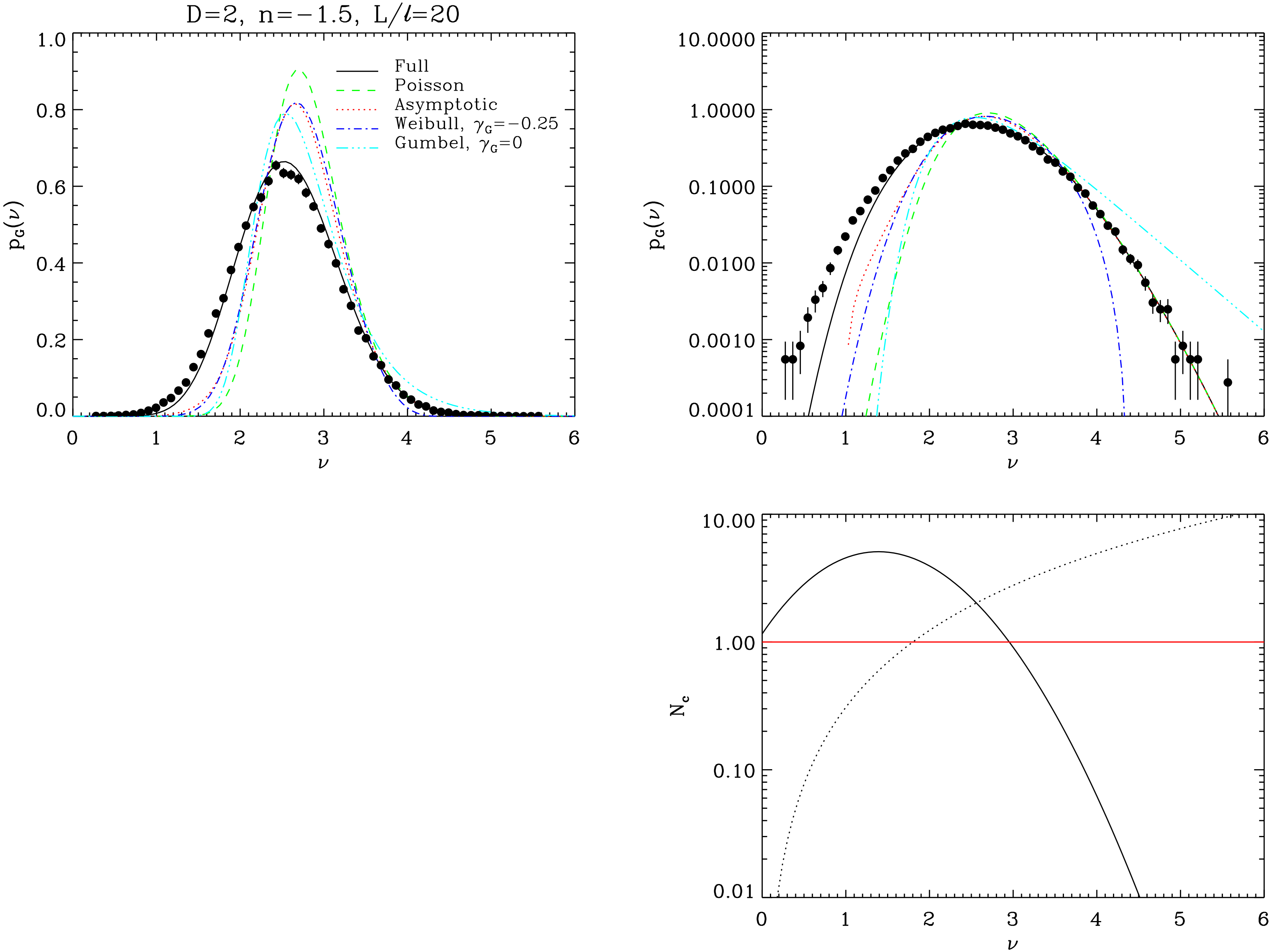

D=2, n=−1.5, L/ℓ=20
Full
Poisson
Asymptotic
Weibull, γG=−0.25
Gumbel, γG=0
pG(ν)
ν
Nc

Example : the CMB extreme value distribution is (indeed) well fitted by a negative Weibull with $\gamma_G<0$

Mikelsons, Silk & Zuntz, 2009, MNRAS 400, 898

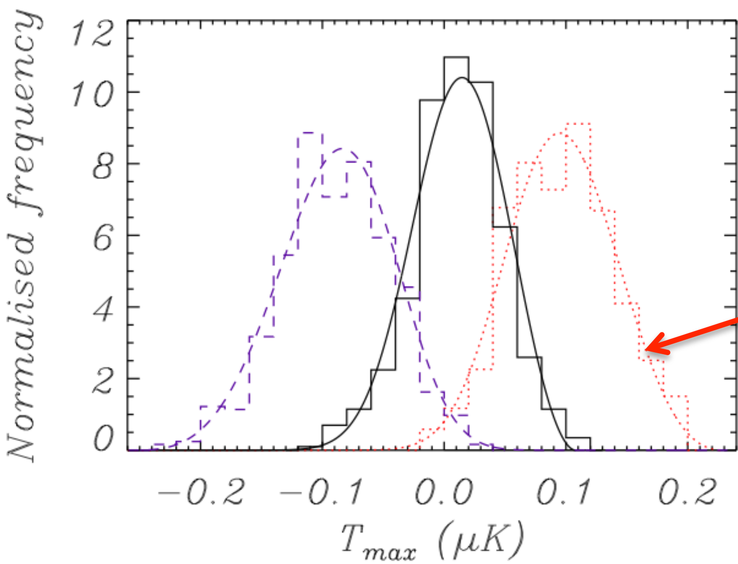

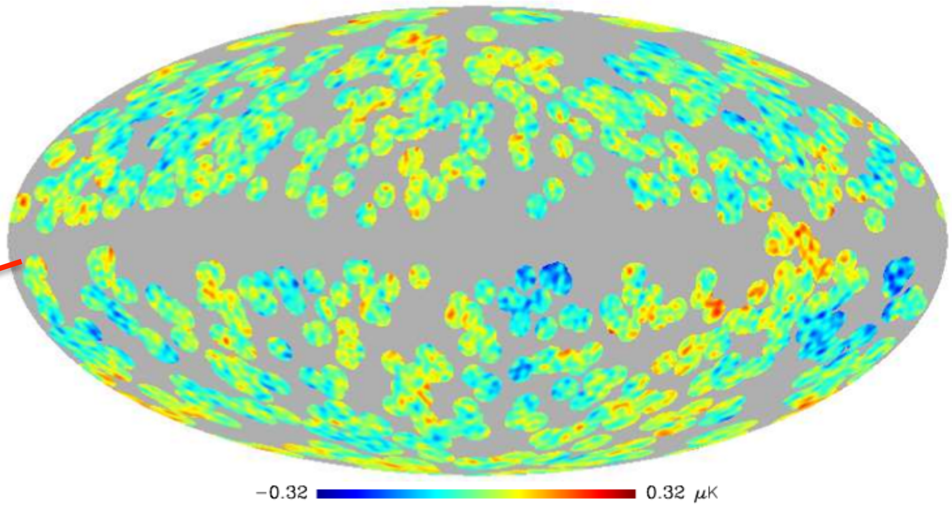

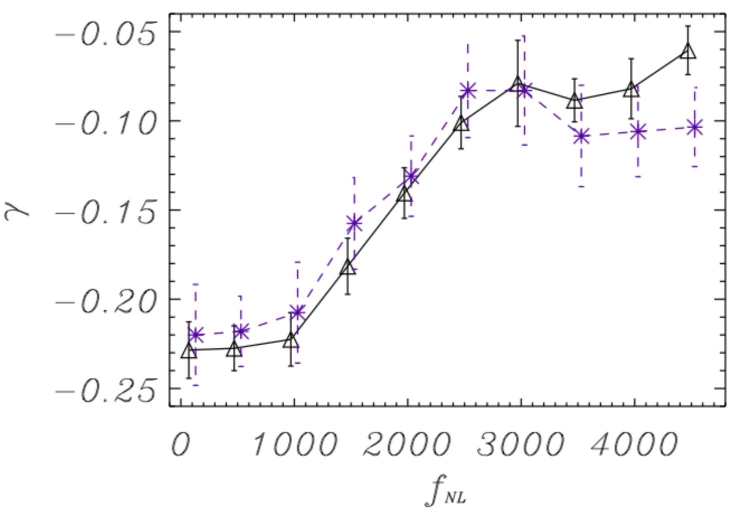

γ_G can be used as a test of the Gaussian nature of the underlying field

f_{NL}: traces the level of skewness

Note: the plot suggests in practice γ_G closer to zero for non Gaussian field than for Gaussian !

Mon. Not. R. Astron. Soc. **417,** 2938–2949 (2011) doi:10.1111/j.1365-2966.2011.19453.x

Note: the case of superclusters

How unusual are the Shapley supercluster and the Sloan Great Wall?

Ravi K. Sheth[1,2]★ and Antonaldo Diaferio[3,4,5]★

[1]*Department of Physics & Astronomy, University of Pennsylvania, 209 S. 33rd Street, Philadelphia, PA 19104, USA*
[2]*The Abdus Salam International Center for Theoretical Physics, Strada Costiera 11, 34151 Trieste, Italy*
[3]*Dipartimento di Fisica Generale 'Amedeo Avogadro', Università degli Studi di Torino, Via P. Giuria 1, I-10125 Torino, Italy*
[4]*Istituto Nazionale di Fisica Nucleare (INFN), Sezione di Torino, Via P. Giuria 1, I-10125 Torino, Italy*
[5]*Harvard–Smithsonian Center for Astrophysics, 60 Garden Street, Cambridge, MA 02138, USA*

Accepted 2011 July 15. Received 2011 July 15; in original form 2011 May 17

ABSTRACT

We show that extreme value statistics are useful for studying the largest structures in the Universe by using them to assess the significance of two of the most dramatic structures in the local Universe – the Shapley supercluster and the Sloan Great Wall. If we assume that the Shapley concentration (volume $\approx 1.2 \times 10^5\,h^{-3}\,\mathrm{Mpc}^3$) evolved from an overdense region in the initial Gaussian fluctuation field, with currently popular choices for the background cosmological model and the shape and amplitude σ_8 of the initial power spectrum, we estimate that the total mass of the system is within 20 per cent of $1.8 \times 10^{16}\,h^{-1}\,\mathrm{M}_\odot$. Extreme value statistics show that the existence of this massive concentration is not unexpected if the initial fluctuation field was Gaussian, provided there are no other similar objects within a sphere of radius $200\,h^{-1}$ Mpc centred on our Galaxy. However, a similar analysis of the Sloan Great Wall, a more distant ($z \sim 0.08$) and extended concentration of structures (volume $\approx 7.2 \times 10^5\,h^{-3}\,\mathrm{Mpc}^3$), suggests that it is more unusual. We estimate its total mass to be within 20 per cent of $1.2 \times 10^{17}\,h^{-1}\,\mathrm{M}_\odot$ and we find that even if it is the densest such object of its volume within $z = 0.2$, its existence is difficult to reconcile with the assumption of Gaussian initial conditions if σ_8 was less than 0.9. This tension can be alleviated if this structure is the densest within the Hubble volume. Finally, we show how extreme value statistics can be used to address the question of how likely it is that an object like the Shapley supercluster exists in the same volume which contains the Sloan Great Wall, finding, again, that Shapley is not particularly unusual. Since it is straightforward to incorporate other models of the initial fluctuation field into our formalism, we expect our approach will allow observations of the largest structures – clusters, superclusters and voids – to provide relevant constraints on the nature of the primordial fluctuation field.

Key words: methods: analytical – galaxies: clusters: general – dark matter – large-scale structure of Universe.

Discussion, perspectives

-**Conclusion**: extreme value statistics can be applied successfully to set interesting constraints on large scale structure formation models, including effects of non Gaussianity

-**Applications** to clusters of galaxies, super-clusters of galaxies, CMB successful or ongoing.

-**Ongoing project:** accurate analysis of the cold spot problem

-**Other possibly interesting applications**
-Largest underdense regions (formerly voids) in the Universe
-Lyman alpha forest ?
-Quasars and other very far and rare objects (e.g. first galaxies)?

OPHYSICAL JOURNAL, 327: L35–L39, 1988 April 15

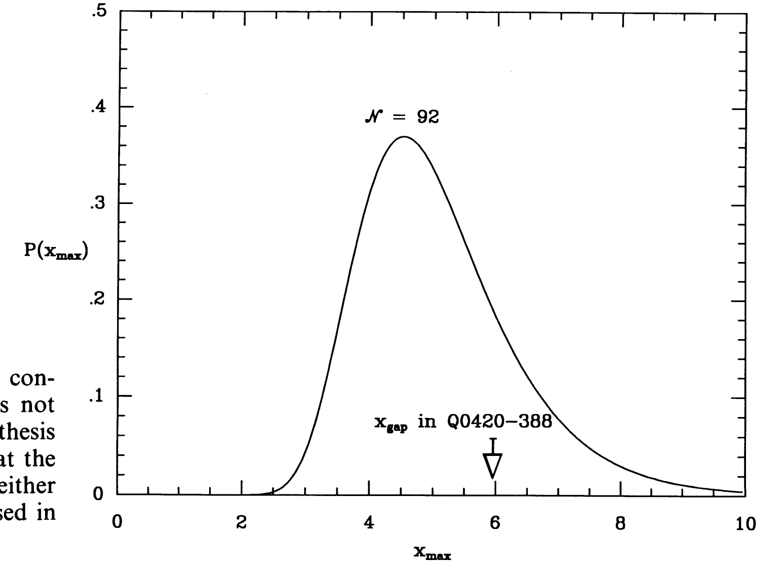

CLUSTERING AND VOIDS IN THE LYMAN-ALPHA FOREST

JEREMIAH P. OSTRIKER, STANISLAW BAJTLIK,[1] AND ROBERT C. DUNCAN
Princeton University Observatory

Received 1987 November 30; accepted 1987 December 30

ABSTRACT

In a statistical study of quasar absorption lines, we find no evidence for large voids in the Lyα forest, contrary to some recent suggestions. The 28 Mpc gap found by Crotts in the spectrum of Q0420−388 is not statistically significant, and we can, from a sample of 18 quasar spectra, reject at the 2 σ level the hypothesis that comoving voids of 30 Mpc fill as much as 15% of the universe. We do, however, find a significant (at the 99% level) excess of small line intervals of velocity width $\Delta v \approx$ 200–600 km s^{-1}. This provides evidence either for the gravitationally induced correlations proposed in some models or for the fragmented shells proposed in others.

Subject headings: galaxies: clustering — quasars

I. INTRODUCTION

istribution of absorption lines in quasar spectra con-
formation about the arrangement of matter on very
ales. Recently, several authors have analyzed Lyα forest
see if they show any structure of size $\sim 50 h_0^{-1}$ Mpc
ng), where h_0 is the Hubble constant in units 100 km
c^{-1}. This is a pertinent question since voids and super-
of such large dimension have been detected in deep
surveys (e.g., Kirshner *et al.* 1981; Davis *et al.* 1982; de
ent, Geller, and Huchra 1986; Haynes and Giovanelli
arswell and Rees (1987) studied the distribution of Lyα
ward Q0420−388 (z_{em} = 3.12) and PKS 2000−330
.78) but found no statistically significant evidence for
^{1} Mpc voids, concluding that the filling factor of such
$f \leq 0.05$. However, Crotts (1987), studying a slightly
dshift range in the lines of sight to the same objects,
ged this result. He found a large void at $z \approx 2.58$ toward
−388 which he calculated was discrepant with the
se locally Poisson-like distribution at the 99% level,
ch gave a measured f marginally inconsistent with the
of Carswell and Rees (1987).
s *Letter* we show that the line interval found by Crotts
ctually discrepant, and that there is as yet no com-
vidence for the existence of large-scale voids in the Lyα
We base these conclusions on our own compilation of
interval distribution in an 18 QSO sample which
Q0420−388. Although we find no evidence for large
e do find a statistically significant excess of *small* line
s ($R_0 \leq 5h_0^{-1}$ Mpc). This excess may be spurious,

lines (four on one side, two on the other) containing prominent features (rest frame $W \geq 0.50$ Å), so it is not valid to treat the gap as a single $42h_0^{-1}$ Mpc void.

How unusual is this gap? If the line distribution is locally Poisson, then the distribution of intervals (neglecting the depletion of small intervals due to line blending) is

$$P(x) = e^{-x}, \tag{1}$$

where $x \equiv \Delta z/\overline{\Delta z}$ is the line interval scaled to the local mean. One can approximate, in any given redshift range,

$$(\overline{\Delta z})^{-1} \equiv \frac{d\mathcal{N}}{dz} = \mathscr{A}(1+z)^{\gamma}, \tag{2}$$

where $\mathscr{A}$ and γ are fitting constants (Murdoch *et al.* 1986, and references therein). Then from equation (1) it can be shown that, in a Poisson sample of $\mathcal{N}$ line intervals, the probability distribution for the *maximum* interval is

$$P(x_{max}) = \mathcal{N} e^{-x_{max}}(1 - e^{-x_{max}})^{\mathcal{N}-1}. \tag{3}$$

Although line blending does not affect the distribution of intervals at large x (eq. [1]), it *does* affect the fitting constants $\mathscr{A}$ and γ (A. P. S. Crotts, private communication). Analyzing an 18 QSO sample complete to rest frame equivalent width W_c = 0.36 Å (Bajtlik, Duncan, and Ostriker 1988), we estimate that the index γ describing the *preblended* line population is 2.84 ± 0.45 (about 0.4 *larger* than the observed, blended value) due to the fact that lines are more crowded at high z. (This assumes a dimensionless blending-strength $\zeta = 2.5$; see § III.) Of course, pairs of close lines that are both below the cutoff W_c